FINAL REPORT
MARCH 1965

CRACK INITIATION IN METALLIC MATERIALS

BY

V. WEISS
G. NASH
K. SCHRODER

FOR

DEPARTMENT OF THE NAVY
BUREAU OF NAVAL WEAPONS
WASHINGTON 25, D.C.

CONTRACT NO. NOw-64-0275-d

SYRACUSE UNIVERSITY RESEARCH INSTITUTE

DEPARTMENT OF CHEMICAL ENGINEERING AND METALLURGY
MET. E. 1160-0365F

CRACK INITIATION IN METALLIC MATERIALS

BY

V. WEISS
G. NASH
K. SCHRODER

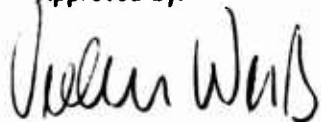# SYRACUSE UNIVERSITY RESEARCH INSTITUTE

DEPARTMENT OF CHEMICAL ENGINEERING AND METALLURGY

Approved by:

VOLKER WEISS

Sponsored by:

DEPARTMENT OF THE NAVY
BUREAU OF NAVAL WEAPONS

S.U.R.I. Report No. MET. E 1160-0365F

Date: MARCH 1965

ABSTRACT

Crack initiation and propagation under alternating loading has been
investigated for a number of technical alloys (AISI 301, PH-15-7Mo, D6-AC,
HP9-4-25, Ti-6Al-4V). The parameters n^+ and N_o relating to the crack
propagation and initiation respectively have been introduced through the
use of a crack propagation law suggested by Weiss and have been correlated
with the specimen geometries and material properties. The parameter n^+ is
thought to depend in some way on the strain hardening coefficient of the
material and is found to provide an indication of the material's resistance
to fatigue crack propagation. The parameter N_o is related to the crack
initiation times and a relation between N_o, the geometry of the specimen,
and the parameter n^+ has been proposed.

i

TABLE OF CONTENTS

LIST OF TABLES

LIST OF FIGURES

LIST OF FIGURES

LIST OF FIGURES

vi

INTRODUCTION

The purpose of the present study is to attempt to ascertain the conditions required for crack initiation and propagation in metallic materials. The process of fracture usually occurs in three distinct stages: the formation of a crack form an existing crack or surface flaw, a period of slow propagation if the material has some ductility, and cataclysmic failure. Most studies to date have been concerned with the last stage (1-6) i.e. cataclysmic failure. This is the area in which fracture mechanics such as the Griffith-Irwin approach (3) and the maximum fracture strength concept (7-9) have been applied with a great deal of success. In either analysis the event of fracture is characterized by a critical stress or energy state. It is therefore reasonable to assume that the two earlier stages, namely crack initiation and crack propagation, should also be analyzable in similar terms. No such unified analysis has been developed to date, although the work of Paris (10), Liu (11), and Weiss (12) on fatigue crack propagation indicates the feasibility of such an approach.

On the microscopic scale the problem involves dislocation mechanics, or more specifically the conversion of glide dislocations to cavity dislocations. This problem has been studied by Petch, Cottrell and others (13, 14, 15, 16) who have postulated a number of such dislocation models. Most of these studies have been concerned with smooth specimens in which the dislocation arrangements could be readily made visible by etch pit or x-ray techniques. Lithium fluouride and silicon iron are favorites among the materials for these studies. An extension of these studies to investigate the initiation

1

of cracks at the base of some milder stress concentrations such as exter-
nally introduced notches was conducted at Syracuse under the present re-
search efforts. A detailed report on the results was presented in interim
technical report No. 1 (17). A brief summary of the results of these
microscopic studies of crack initiation is given below.

LiF crystals could fracture at surface irregularities or by an internal
slip band mechanism. The latter process occurred in the compression of
highly polished specimens. In that case, it seemed to be necessary that
cracks were nucleated at slip band intersections. Surface steps such as
slip steps were also responsible for crack initiation in highly polished
crystals. The first cracks nucleated at the base of slip steps either as
(100) or (110) cracks and propagated in the interior.

A moderately clean surface presents a barrier to the emergence of dislo-
cations. There is no preferred site for slip bands. If two conjugate slip
bands force dislocations against this barrier slightly below the surface
a crack nucleates on a (100) plane as predicted in a crack mechanism by
Cottrell (18). With only one active slip band, the crack initiation seemed
to follow a model suggested by Gilman (19). Again the crack was formed at
the barrier below the surface and propagated into the remaining material.
Similar results were obtained on notched specimens. The crack did not start
at the point with the highest geometrical stress concentration, but several
microns below the surface in an area surrounding the notch root.

An examination of the (100) cracks on the (100) faces reveal a small
volume element immediately at the crack tip with a nearly uniform dislocation
distribution. Parallel sets of edge dislocations with [110] and [110] Burger's

2

vectors seem to emanate from the tip of the crack. On adjacent (010) planes examined after the specimen had been separated into two parts, a series of screw dislocations were observed in the vicinity of the previously stopped crack. These screw dislocations have Burger's vectors in (110) and (1$\bar{1}$0) planes. This appears to justify the assumption that simple edge-screw loops emerge or move into the tip of the crack.

It was attempted in the LiF studies to correlate these dislocation structures with theories which are used to analyze the fracture process. Plots of gross section strength vs. notch depth were made to obtain the plasticity correction (ASTM Fracture Committee) or the particle size η respectively. It was found in each case that the area near the crack tip with the high nearly uniform dislocation density had a size of the order of η , or the plastic zone.

The present report describes the study of crack initiation and propagation behavior of technical alloys under alternating stress systems. This approach was chosen because it is hoped that from extrapolation of the notch fatigue curves to zero crack extension, some insight could be gained about the factors responsible for crack nucleation from an existing notch. Furthermore, the propagation of an existing fatigue crack constitutes a continued reinitiation process. Thus it is hoped that an analysis of such notch fatigue data obtained under carefully controlled conditions will yield information concerning the initiation and propagation of cracks in technical materials.

The materials selected for this study include high strength steels, (HP9-4-25, D6AC), austenitic stainless steels (AISI 301), precipitation

3

hardening stainless steels (PH-15-7Mo in the CH900 and RH1050 conditions), and the titanium alloy RS-120 (Ti-6Al-4V in the annealed condition). Since the ductility of the material was suspected to have a strong influence on the crack initiation and propagation behavior, stress-strain base data and static notch-tensile data were obtained for all these materials. Three test series to determine the crack initiation and propagation conditions of notch specimens were contemplated:

1. <u>Constant applied net section stress.</u> Here the effect of stress concentration factor only, between 3.1 and 17, would be obtained on the initiation and propagation resistance.

2. <u>Constant maximum stress at the notch root.</u> Here the net section stress times the elastic stress concentration factor was held constant, thus all specimens would have experienced the same stress at the root of the notch under elastic conditions.

3. <u>Maximum net section stress at a constant fraction of the experimentally observed notch strength</u> as a function of stress concentration factor. Here the stress amplitude decreased with increasing stress concentration factor but at a lesser rate than for series 2. The maximum net section stress values of this series would lie on a straight line parallel to the log. σ_N vs log K_t curve obtained in monotonic tension.

In addition, crack propagation data were obtained on sharp notch $(K_t = 17)$ specimens of PH-15-7Mo and Ti-6Al-4V. All tests were to be conducted with a minimum net section stress very slightly above zero, i.e.

$$r = \sigma_{Min} / \sigma_{Max} \simeq 0$$

The objective of the first series is to determine the connection between the stress concentration and crack initiation time. The second series is a check on the applicability of linear elastic analysis on crack initiation in technical materials. The last series should provide information concerning the connection between static fracture and fatigue crack initiation and propagation. To date primarily tests of series number 3 have been completed together with tests on crack propagation rate as a function of the strain hardening characteristics of the material. Completion of test series 1 and 2 as well as a detailed investigation of the crack initiation conditions under monotonic tensile loading is contemplated for the continuation effort. In addition to notch geometry; the environment, the test rate, and the test temperature will constitute experimental variables.

EXPERIMENTAL PROCEDURE

Notch sheet specimens of Republic HP9-4-25, D6AC, AISI 301 stainless, titanium RS-120 (annealed), and PH-15-7Mo (CH 900 and RH 1050) were prepared with stress concentration factors ranging from 3.1 to 17. Fig. 1 is an illustration of the test specimen and gives the critical dimensions as a function of stress concentration factors. The titanium specimens and the PH-15-7Mo CH900 and RH 1050 specimens all had stress concentration factors of 17. The stress concentration factors of the specimens from the other materials were 3.1, 4.1, 7.3, 19.4 and 17.

The ultimate tensile strength and the "n" values for these materials are given in Table 2. The effects of the elastic stress concentration factor on the notch strength, as obtained under static testing conditions, for D6AC, HP9-4-25 and AISI 301 are illustrated in Figures 2-4 and the results are also listed in Table 3. It should be noted that these σ_N-K_t curves in a log-log representation constitute nearly straight lines according $\sigma_N \cdot K_t^m$ = const. Neuber's relationship between stress concentration factor, K_σ, strain concentration factor, K_ϵ, and elastic stress concentration factor, K_t; $K_\sigma \cdot K_\epsilon = K_t^2$ leads, together with the assumption of an experimental strain hardening behavior $\sigma = C\epsilon^n$ to the relationship const. $= \sigma_N \cdot K_t^{2n/n+1}$ which is in qualitative agreement with the observed results. Thus the slopes of the σ_N-K_t curves can also be utilized to determine a "n" value for the material. This latter value should be regarded as a derived value and will be indicated by an asterisk, n*, in future references. These values themselves are also given in Table 2.

6

The results of these tests allow the design of test series number 3. In this test series, the mean stress was .55 $\sigma_{N, Max}$ in order to allow a slight tension stress at the minimum stress amplitude. Crack growth was recorded photographically.

During the fatigue crack propagation process the load carrying cross-section, or area of the specimen, decreases and hence the nominal load increases. As in the Sonntag machine the mean load is applied by a spring and therefore tends to relax with crack propagation, it was necessary to obtain a calibration of the true net section stress as a function of the crack length. To obtain this calibration, the load drop was determined as a function of crack length during actual fatigue tests on an instrumented specimen. The effects of the nonhomogeneity of the stress fields at the location of the strain gages were eliminated by another calibration series. The calibration curve which gives the strain reading from the gage mounted to the specimen as a function of the net section stress is given in Figure 5. Figure 6 shows the change in the maximum net section stress during the fatigue testing of a PH15-7-Mo specimen. It is evident that the relaxation of the mean stress compensates to some extent for the decrease in the net cross sectional area. However, a slight increase in net section stress with increasing crack length was observed in all specimens. This point is significant for the future analysis of the experimental results.

7

EXPERIMENTAL RESULTS

Crack propagation curves for AISI 301, 50% cold reduced are shown in
Figures 7-10. Here the log of the total crack length, i.e. the sum of the
initial notch depth and the two edge fatigue cracks is plotted against the
number of cycles. The values of K_t which were used in this test series
were 3.1, 4.1, 9.4, and 17. The net section stress was varied in accordance
with test series 2 for the alternating stress but with a constant mean stress
of 39 ksi. As can be seen form these curves, the relationship between log
total crack length and number of cycles is linear to a good degree of
approximation except for the curve representing a K_t value of 3.1. In this
curve the initial portion seems to deviate from the linearity observed in
the later stages of propagation due to the overlapping effects of the notch
and crack stress fields. In the final stages of propagation for each one of
the curves being discussed, an upswing is observed which is due to the increase
in the true net section stress as shown in Fig. 6.

Crack propagation curves for sharply notched $(K_t = 17)$ sheet specimens of
Ti-6Al-4V, annealed, and Ph-15-7Mo, CH900 and RH 1050 are shown in Figs. 11-20.
Again the longarithm of the total crack length is plotted against the number
of cycles. Each material was tested at several different stress levels
as shown in Table 4. For Ti-6Al-4V, Figs. 11-14, the curves show a linear
trend but the scatter is much greater than that of the preceeding test series.
This may be due to the fact that for this test series the specimens were
cycled from zero to σ_{Max} and thus the crack was nearly closed for part of
each cycle. When the photographs of the cracks from this test series were
examined it was found that the crack tip was not as easily distinguished as

8

in the constant mean stress tests i.e. AISI 301 just discussed. For the

PH-15-Mo specimens , Figs. 15-20 ,the curves better approximate a linear relation

between log total crack length and number of cycles. Since the cycling in this

test series was also zero to σ_{Max} and the same photographic technique was

used for both the RS-120 titanium and the PH-15-7Mo, the explanation for the

deviation from linearity in the Ti-6Al-4V data may not be completely valid.

The crack propagation curves for HP9-4-25 and D6AC as a function of

stress concentration factor in accordance with test series 3, are shown in

Figs. 21-28. Here the ratio C/C_o, where $2C_o$ is initial and $2C$ the instantaneous

crack length, is plotted against the number of cycles in semilogarithmic

coordinates.

The K_t values tested in this series were 3.1, 4.1, 7.3, 9.4 and 17.

The curves for the HP9-4-25,Figs. 21-24, show the same type deviation observed in

the Ti-6Al-4V specimens. Since for the tests on the HP9-4-25 and the D6AC a

stroboscopic flash system was employed so that photographs would only be

taken when the crack was open, it is doubtful that inaccuracies in measurement

of the crack length can explain these deviations. In the curve for K_t=4.1

i.e. Fig. 24, the deviation from linearity seems to take place only in the

initial portion of the curve. This may be explained in the same way as

for the K_t = 3.1 curve for the AISI 301 stainless (Fig. 6). A curve for K_t=3.1 for

the HP-9-4-25 is not shown because it was found that the applied net section

stress was so high that once the crack initiated, it propagated too rapidly

to be photographed using the present experimental set up.

For the D6AC, the curves for the specimens of K_t = 17 and 9.4 show

the same type of deviation from linearity as observed in the Ti-6Al-4V.

9

The curve $K_t = 3.1$ is not shown for this material for the same reason as stated previously for the specimen of HP 9-4-25.

ı

'or

DISCUSSION

A linear relationship between the longarithm of the instantaneous crack length and the number of cycles has been postulated previously (20-24) and justified by Weiss (20) for both strain and stress controlled fatigue. Accordingly

$$\frac{dC}{dN} \approx c\left(\frac{\varepsilon_{TR}}{\varepsilon_F}\right)^{n^+ + 1} \qquad \text{Equ. 1}$$

for strain controlled and

$$\frac{dC}{dN} \approx c\left(\frac{\sigma_{N,\,Max}}{\sigma_F}\right)^{(n^+ + 1)/n^+} \qquad \text{Equ. 2}$$

for stress controlled cycling. Here ε_{TR} is the strain range, ε_F the fracture strain, $\sigma_{N,\,Max}$ the maximum net section cycle stress and σ_F the fracture strength, more specifically the extrapolated value to $K_t = 1$ of the corresponding σ_N-K_t curve.

The second equation, which would apply to the present case, yields

$$\ln \frac{C}{C_o} = A\left(\frac{\sigma_{N,\,Max}}{\sigma_F}\right)^{(n^+ + 1)/n^+} (N-N_o)$$

$$\text{Equ. 3}$$

and one can obtain the n^+ values from the slope of the curves

$$\log \frac{\ln C/C_o}{(N-N_o)} \quad \text{vs} \quad \log \sigma_N, \text{ Max} \qquad \text{Equ. 4}$$

which are illustrated in Figs. 29 to 32. Derived n^+ values from such curves are given in Table 2 together with the n values from stress strain curves and n^* values from $\ln \sigma_N - \ln K_t$ curves. The fatigue "n^+" values

11

are in fair agreement with the n* values, which both are higher than the "n" values obtained from stress-strain diagrams. This may be in part due to the neglecting of the elastic portion of the stress strain curve, i.e. the σ_0 term of $\sigma = \sigma_0 + K_\epsilon^n$.

A further question arises concerning the use of the maximum cycle stress instead of the nominal or net stress range ($2 \sigma_A$) of Fig. 32. Because of the high stress concentration effects of a crack the region near the crack tip must experience considerable compressive stresses in the low tension part of the cycle, hence the use of $2\sigma_A$ appears more justified than the use of the nominal or net maximum cycle stress. In other words, the net stress ratio $R_{net} = \sigma_{Min}/\sigma_{Max} = 0$ may well produce a true stress ratio near the root of a crack $R_{true} = \sigma_{Min}/\sigma_{Max}$ (at crack tip) $\approx$ -1. For test series in which $R_{net} = 0$ the n^+ values are not affected by these considerations. However, for test series with a constant mean stress, different n^+-values are obtained depending on the choice of σ_{Alt} or σ_{Max}. This is illustrated by the data of Fig. 7-10, Fig. 32 on AISI 301 stainless and the data recently obtained by NASA Langley (25). A plot of log $\sigma_{N, Max}$ or log σ_A vs log N for a given percent crack growth should yield the value of $n^+/(n^+ + 1)$. This can readily be seen from Equation 3 since for an assumed incremental crack growth $\ln \dfrac{C}{C_0}$ = constant and it follows that

$$[(N-N_o)^{\, n^+/(n^+ + 1)}] \; \sigma_{N,Max} = \text{const.}$$

Equ. 5

which yields $(n^+/n^+ + 1)$ as the negative slope of the σ_{Alt} vs $(N-N_o)$ curves.

The results of the room temperature data reported by Hudson lend

12

themselves readily to such an analysis. Fig. 33 is a replot of the NASA data in the proposed log C vs N form. It can be seen that straight line relationships result for AM-350, AM-367 and Ti-8Al-1Mo-1V in the 0.050 in. thick material while an upward curvature is observed for the remainder of the materials. This may indicate a deviation from the proposed propagation relationship and may also in part be due to sheet thickness (especially for Ti-8Al-1Mo-1V, 0.250 in. thick) and to the net section stress increase as the crack growth progresses. Nevertheless, any propagation law of the form

$$\frac{dC}{dN} = f\ (C)\ \cdot\ (\sigma)^{\alpha}$$

leads to a relationship of the type of Equation 5. Figs. 34 to 40 show Hudson's data in this representation. The derived n^+ values again depend on whether the maximum cycle stress or the alternating stress is chosen for the representation. Table 5 gives the n^+ values for this data. The reasons for the variation of these n^+ values and their dependence on the choice between the alternating stress and the mean stress are not clear at present. An analysis of these effects may, however, lead to a deeper understanding of the plastic flow problem near the tip of a crack subjected to alternating stresses.

Since an increase in the n^+ value indicates an increase in crack propagation rate in stress controlled fatigue tests, materials may be rated for their fatigue resistance on that basis. The observation of large n^+ values close to unity is reminiscent of the results obtained under strain cycling (12). It seems, therefore, that with increasing n^+ values the crack propagation becomes more and more a strain controlled process occurring near the tip of the crack.

13

The initiation of cracking from a notch can be analyzed in terms of the N_o values, i.e. the values of the intercept of the straight log C vs N line at zero crack extension from the notch. These values are tabulated in Table 4. The information available on stress and strain fields near a notch (Grewal, Weiss ASM Strain Concentrations) allows a simple analysis of this problem. The tentative assumption is made that the material ahead of the notch experiences strain cycling and that the crack initiation time is a function of the strain history in a small region ahead of the crack of the type

$$N_o^\alpha \, \epsilon_p = \text{constant} \qquad \text{Equ. 6}$$

Both the constant on the right hand side of Equation 6 and the exponent α are postulated as material characteristics. The strain amplitude ahead of the notch can be obtained from Neuber's relationship (26),

$$K_\sigma \cdot K_\epsilon = K_t^2 \qquad \text{Equ. 7}$$

and yields, for exponential strain hardening

$$\epsilon_p = \epsilon_N \cdot K_\epsilon = \left(\frac{\sigma_N}{E}\right) K_t^{2/(n^+ + 1)} \qquad \text{Equ. 8}$$

For the ideally plastic case, n = 0 near the notch root one obtains

$$(N_o \, K^2) \, \sigma_N = \text{constant} \qquad \text{Equ. 9}$$

A more complete analysis, utilizing the crack propagation relationships proposed by Weiss (12, 20) yields

$$(N_o \, K_t^2)^{\frac{1}{n^+ + 1}} \, \sigma_N = \text{constant} \qquad \text{Equ. 10}$$

14

Fig. 41 is a plot of $\sigma_{N,Max}$ or $\sigma_{N, Alt}$ as a function of $(N_o K_t^2)$ in log-log coordinates. It can be seen that all results obtained in this study fall in a scatterband having a slope of approximately 0.21. This leads to an n-value in excess of 1, namely approximately 3.7, which is not readily acceptable. If, however, one considers the crack initiation process as a build up of microscopic events including the development of residual stresses etc., in the triaxial stress field ahead of a notch, a stress—strain relationship which is convex towards the strain axis may not be totally unreasonable. More work, especially on crack initiation under monotonic loading,is required to resolve this question. The fact that the choice of $(N_o K_t^2)$ as the abcissa leads to a single relationship must not be overlooked.

SUMMARY AND CONCLUSIONS

As a result of the experimental work performed in this study, the
following conclusions may be drawn:

1) Crack propagation under alternating loading is related in some way
to the stress-strain characteristics of the material in both the elastic
and the plastic range.

2) A simplified analysis of crack propagation using a maximum stress fracture
concept yields n^+ values which provide an indication of the material's
resistance to slow crack growth, i.e. $\frac{dC}{dN}$ increases with increasing n^+. The
value of n^+ is thought to be related to the strain hardening coefficient
calculated from monotonic tensile tests.

3) A question arises as to the correct stress range in the region near
the crack tip. As pointed out earlier, if the nominal stress range is
zero, the stress range near the crack tip may be close to -1. This
effect leads to an ambiguity in the determination of n^+ for test series
in which the nominal stress range is unequal to zero. As of now, it is
not clear as to how to take this effect into account.

4) The data recently obtained at NASA Langley fits the analysis
presented here since the n^+ values obtained agree closely with the n^+
values in the present study. Also, the same ambiguity is found in the
determination of the n^+ values due to the stress range being unequal to zero.

5) A simplified analysis of the process of crack initiation from a pre-
existing notch or crack assuming that a volume element at the crack tip
undergoes strain cycling predicts the general trend of N_o as a function of

16

K_t and σ nominal. The n^+ values predicted by this analysis however are exceedingly high and thus this analysis is probably not completely valid. As mentioned at the end of the discussion however, the choice of $K_t^2 \, N_o$ as the abcissa of the $\sigma_{N, \, Max}$ vs. $K_t^2 \, N_o$ curve tends to place all the data on a single line. Whether this is strictly fortuitous or is an indication that this analysis is headed in the right direction is not known at present. It appears that only a better understanding of the stress and strain states at the notch root during alternating loading will provide the answer to this question.

17

REFERENCES

1. A. A. Griffith, "The Phenomena of Rupture and Flow in Solids," Roy. Soc. London Phil Trans. Series A, Vol 220 (1920), pp. 163-198

2. E. Orowan, "Fracture and Strength of Solids", Report on Progress in Physics, Phys. Soc. London, Vol 12 (1949) p. 185

3. G. R. Irwin, "Fracture", Springer "Encyclopedia of Physics," Vol 6, 1958, pp. 551-590

4. B. L. Averbach, D. K. Felbeck, G. T. Hahn, D. A. Thomas, eds., "Fracture," J. Wiley, New York (1959)

5. D. C. Drucker and J. J. Gilman, eds., "Fracture of Solids," J. Wiley, New York (1962)

6. ASTM Symposium on Fracture Toughness Testing and Its Applications, Chicago, June 23-24, 1964

7. V. Weiss, "Current Views and Theories on Fracture", "Crack Initiation and Propagation," presented at Seventh Sagamore Conference (1960), Syracuse Univ. Met E 661-ISIIF (1961)

8. V. Weiss, J. G. Sessler, and G. Sachs, "Analysis of Brittle Fracture in Sheet Materials," MAB Symposium on "Design with Materials that Exhibit Brittle Behavior," MAB-175-M., Vol 1, (1961)

9. V. Weiss and J. G. Sessler, "Analysis of Effects of Test Temperature on the Notch Strength of High-Strength Sheet Alloys", ASTM Special Technical Publication No. 302 (1961)

10. P. C. Paris, "The Fracture Mechanics Approach to Fatigue," in "Fatigue-An Interdisciplinary Approach," J. J. Burke, N. L. Reed, V. Weiss, eds., Syracuse University Press (1964)

11. H. W. Liu, "Fatigue-An Interdisciplinary Approach," S.U. Press (1964) pp. 127-131

12. V. Weiss, "Analysis of Crack Propagation in Strain-Cycling Fatigue," in "Fatigue-An Interdisciplinary Approach," S. U. Press (1964)

13. N. J. Petch, "The Ductile-Cleavage Transition in Alpha-Iron," in "Fracture," J. Wiley, New York (1959)

14. A. H. Cottrell, "Theoretical Aspects of Fracture," in "Fracture," J. Wiley, New York (1959)

18

15. J. Friedel, "The Propagation of Cracks and Work Hardening," in "Fracture," J. Wiley, New York (1959)

16. A. S. Tetelman, "The Plastic Deformation at the Tip of a Moving Crack," in "Fracture of Solids," J. Wiley, New York (1962)

17. P. Packman, K. Schroder, V. Weiss, "Crack Initiation in Crystalline Materials," Interim Technical Report No. 1 under Contract NOw 64-0275-d (1964)

18. A. H. Cottrell, Trans AIME, Vol 212 (1958) p. 192

19. J. J. Gilman, Trans AIME, Vol 212 (1958) p. 783

20. V. Weiss and J. G. Sessler, "Strain-Controlled Fatigue in Pressure Vessel Materials," ASME Paper No. 63-WA-226 (1963)

21. N. E. Frost and D. S. Dugdale, "The Propagation of Fatigue Cracks in Sheet Specimens," J. Mech. and Phys. of Solids, Vol 6, (1958), No 2

22. H. W. Liu, "Crack Propagation in Thin Metal Sheet under Repeated Loading," Trans ASME, Vol 83 (1961), pp. 23-31

23. S. R. Valluri, "Some Recent Developments at "GALCIT" Concerning a Theory of Metal Fatigue," Acta Metallurgica, Vol 11 (1963) pp. 759-776

24. S. R. Valluri, " A Unified Engineering Theory of High Stress Level Fatigue," Aerospace Engineering Review, (Oct, 1961)

25. C. M. Hudson, "Studies of Fatigue Crack Growth in Alloys Suitable for Elevated-Temperature Applications," NASA TN D-2743

26. H. Neuber, "Research on the Distribution of Tension in Notched Construction Parts," WADD TR 60-906 (1961) and Summary Report to ASD (1962)

TABLE 1

CHEMICAL COMPOSITIONS OF MATERIALS TESTED

ELEMENT	AISI 301 PERCENT MIN	MAX	PH-15-7Mo PERCENT MIN	MAX	D6AC PERCENT MIN	MAX	HP-9-4-25 PERCENT MIN	MAX	RS-120 PERCENT MIN	MAX
CARBON	-	0.15	-	0.09	0.42	0.48	0.24	0.30	-	0.10
MANGANESE	-	2.00	-	1.00	0.60	0.90	0.15	0.35	-	-
SILICON	-	1.00	-	1.00	0.15	0.30	-	0.35	-	-
PHOSPHOROUS	-	0.045	-	0.04	-	-	-	0.01	-	-
SULFUR	-	0.03	-	0.03	-	-	-	0.01	-	-
CHROMIUM	16.00	18.00	14.00	16.00	0.90	1.20	0.35	0.55	-	-
NICKEL	6.00	8.00	6.50	7.75	0.40	0.70	7.50	9.00	-	-
MOLYBDENUM	-	-	2.00	3.00	0.90	1.10	0.35	0.55	-	-
ALUMINUM	-	-	0.75	1.50	-	-	-	-	5.50	6.75
IRON	BALANCE		BALANCE		BALANCE		BALANCE		-	0.30
COBALT	-	-	-	-	-	-	3.50	4.50	-	-
VANADIUM	-	-	-	-	0.05	0.10	0.06	0.12	3.50	4.50
OXYGEN	-	-	-	-	-	-	-	-	-	0.20
NITROGEN	-	-	-	-	-	-	-	-	-	0.05
HYDROGEN	-	-	-	-	-	-	-	-	-	0.15
TITANIUM	-	-	-	-	-	-	-	-	BALANCE	

TABLE 2

THE CONDITION, STATIC TENSILE PROPERTIES, AND "n" VALUES FOR THE MATERIALS TESTED

Material	Condition	UTS	σ_F	n	n^*	n^+_1	n^+_2
AISI 301	51% COLD REDUCED	230 KSI	280 KSI	.08	.055	.18	1.0
HP9-4-25	1550°F(30)OQ-475°F (2)-AC-475°F(2)-AC		390 KSI	-	.202	.37	.37
D6AC	1550°F(30)-1050°F(30) OQ-475°F(2)-AC 475°F(2)AC		350 KSI	-	.165	.22	.22
RS-120	ANNEALED	135 KSI	-	.12	-	1.0	1.0
PH-15-7Mo CH 900	SOLUTION TREATED 900°F(1)-AC	280 KSI	-	.27	-	.80	.80
PH-15-7Mo RH 1050	1750°F(10), AC to 75°F IN 1 HR -110°F(22 HRS) AIR WARMED TO 75°F, 1050°F(1)-AC	200 KSI	-	.01	-	.80	.80

NOTES:

1) n^+_1 IS THE VALUE OF n^+ OBTAINED USING σ_N, MAX n^+_2 IS THE VALUE OBTAINED USING σ_N, ALT

2) THE n VALUE FOR THE AISI 301 WAS OBTAINED FROM THE STRESS-STRAIN CURVE OF A SMOOTH SPECIMEN. THE n VALUES OF THE PH-15-7Mo AND THE RS-120 WERE OBTAINED BY THE _____ METHOD.

TABLE 3

STATIC NOTCH STRENGTH DATA

MATERIAL	K_t	NOTCH STRENGTH
AISI 301	17	200 KSI
	9.4	212 KSI
	7.3	225 KSI
	4.1	238 KSI
	3.1	240 KSI
HP 9-4-25	17	162 KSI
	9.4	186 KSI
	7.3	171 KSI
	4.1	249 KSI
	3.1	262 KSI
D6AC	17	164 KSI
	9.4	177 KSI
	7.3	199 KSI
	4.1	249 KSI
	3.1	251 KSI

TABLE 4

TEST LOADS AND N_0 VALUES

MATERIAL	K_t	No (CYCLES)	ALTERNATING STRESS σ_N, ALT	MEAN STRESS σ_N, mean	MAXIMUM STRESS σ_N, max	CYCLES TO FAILURE (N_F)
AISI-301	17	37,000	± 7.4 KSI	39.0 KSI	46.4 KSI	20,550
	9.4	8,500	± 13.0 KSI	39.0 KSI	52.0 KSI	18,750
	7.3	-	± 16.0 KSI	39.0 KSI	55.0 KSI	-
	4.1	7,000	± 30.0 KSI	39.0 KSI	69.0 KSI	73,850
	3.1	15,050	± 35.0 KSI	39.0 KSI	74.0 KSI	250,900
HP-9-425	17	6,800	± 20.4 KSI	25.0 KSI	45.4 KSI	22,850
	9.4	2,900	± 25.0 KSI	30.5 KSI	55.4 KSI	10,250
	7.3	3,700	± 27.2 KSI	33.2 KSI	60.4 KSI	8,950
	4.1	6,500	± 32.9 KSI	40.2 KSI	73.1 KSI	9,000
	3.1	-	± 36.0 KSI	44.0 KSI	80.0 KSI	-
D6AC	17	9,200	± 20.8 KSI	25.4 KSI	46.2 KSI	22,500
	9.4	4,400	± 24.6 KSI	30.1 KSI	54.7 KSI	10,500
	7.3	7,000	± 26.6 KSI	32.2 KSI	58.8 KSI	9,900
	4.1	8,200	± 31.2 KSI	38.0 KSI	69.2 KSI	10,900
	3.1	-	± 33.8 KSI	41.2 KSI	75.0 KSI	-
RS-120	17	52,000	± 10.0 KSI	12.2 KSI	22.2 KSI	116,100
	17	14,000	± 11.5 KSI	14.1 KSI	25.6 KSI	67,600
	17	7,100	± 14.3 KSI	17.5 KSI	31.8 KSI	33,400
	17	12,100	± 14.6 KSI	17.8 KSI	32.4 KSI	32,600
	17	1,500	± 29.2 KSI	35.8 KSI	65.0 KSI	7,500
	17	1,500	± 29.7 KSI	36.3 KSI	66.0 KSI	7,500
PH-15-7Mo (CH 900)	17	26,000	± 12.6 KSI	15.4 KSI	28.0 KSI	106,200
	17	9,000	± 15.6 KSI	19.0 KSI	34.6 KSI	56,600
	17	8,900	± 19.0 KSI	23.1 KSI	42.1 KSI	35,250
PH-15-7Mo (RH-1050)	17	20,500	± 19.0 KSI	15.5 KSI	34.5 KSI	59,100
	17	6,400	± 23.1 KSI	18.9 KSI	42.0 KSI	32,100
	17	5,100	± 25.3 KSI	20.8 KSI	46.1 KSI	32,800

NOTE:

THE N_0 AND N_F VALUES ARE AVERAGE VALUES COMPUTED FROM THE
RESULTS OF BETWEEN TWO AND FOUR TESTS AT EACH STRESS LEVEL.

TABLE 5

NASA DATA

MATERIAL	THICKNESS	MEAN STRESS	ALTERNATING STRESS	n^+_1	n^+_2	UTS
AM 350 (CRT)	0.050 IN	40 KSI	60KSI, 40KSI, 20KSI 10KSI, 5KSI	0.26	1.0	223.4 KSI
AM 367	0.050 IN	40 KSI	40KSI, 20KSI, 10KSI	0.148	0.61	243.4 KSI
INCONEL 718	0.050 IN	40 KSI	60KSI, 40KSI, 20KSI 10KSI, 5KSI	0.30	0.65	193.7 KSI
Ti-8Al-1Mo-1V DUPLEX ANN	0.250 IN	25 KSI	25KSI, 15KSI, 10KSI 5KSI, 2KSI	0.11	0.44	137.4 KSI
Ti-8Al-1Mo-1V DUPLEX ANN	0.050 IN	25 KSI	25KSI, 15KSI, 10KSI 5KSI, 2KSI	0.164	0.80	152.0 KSI
2020-T6 ALUMINUM	0.050 IN	15 KSI	15KSI, 10KSI, 5KSI 3.5KSI, 2KSI	-	-	81.8 KSI
2024-T81 (CLAD) AL	0.063 IN	15 KSI	15KSI, 10KSI, 5KSI 3.5KSI, 2KSI	0.13	0.57	63.2 KSI
RR-58 (CLAD) ALUMINUM	0.063 IN	15 KSI	15KSI, 10KSI, 5KSI 3.5KSI, 2KSI	0.14	0.57	59.2 KSI

NOTE:

1) n^+_1 IS THE VALUE OF n^+ OBTAINED USING σ_N, MAX
   n^+_2 IS THE VALUE OBTAINED USING σ_N, ALT
2) SPECIMENS IN THIS TEST WERE CENTER NOTCHED WITH 8 IN.CROSS SECTIONS
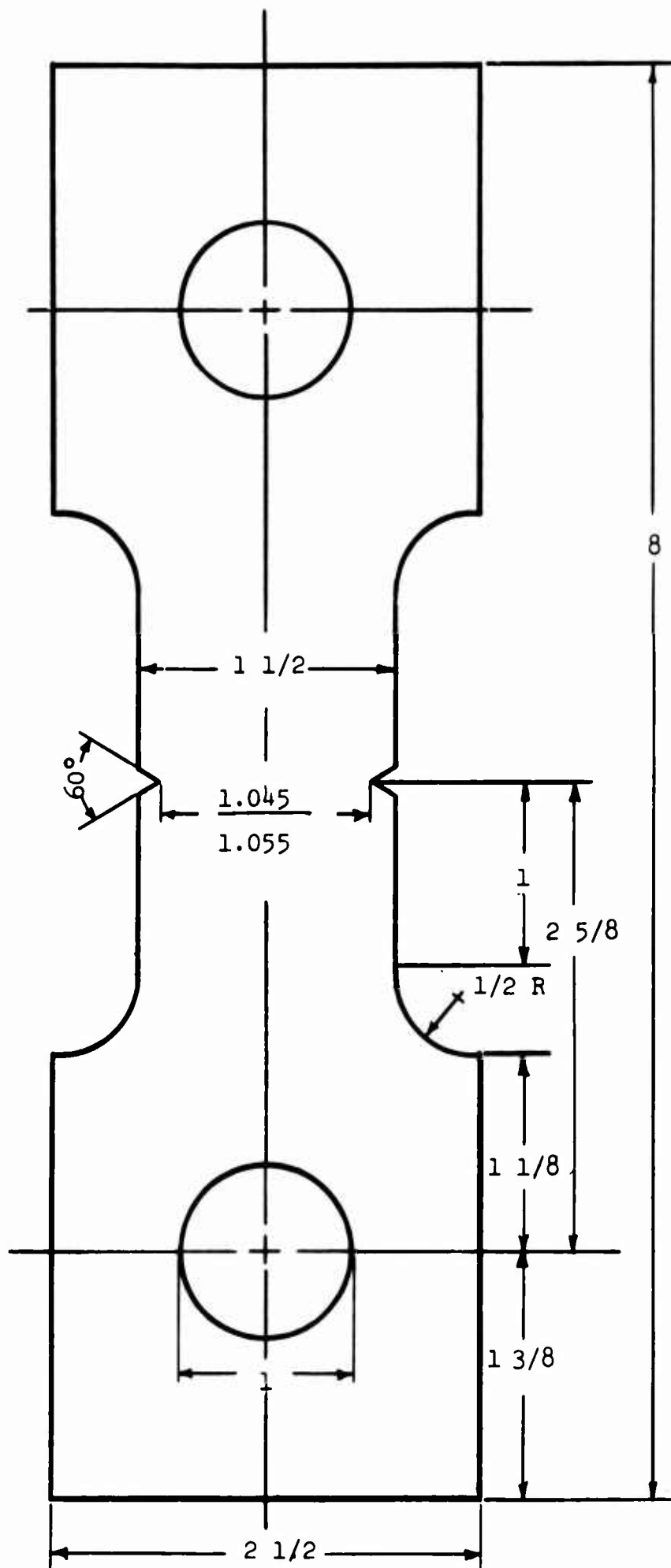
FIG. 1 NOTCH SHEET FATIGUE TEST SPECIMEN
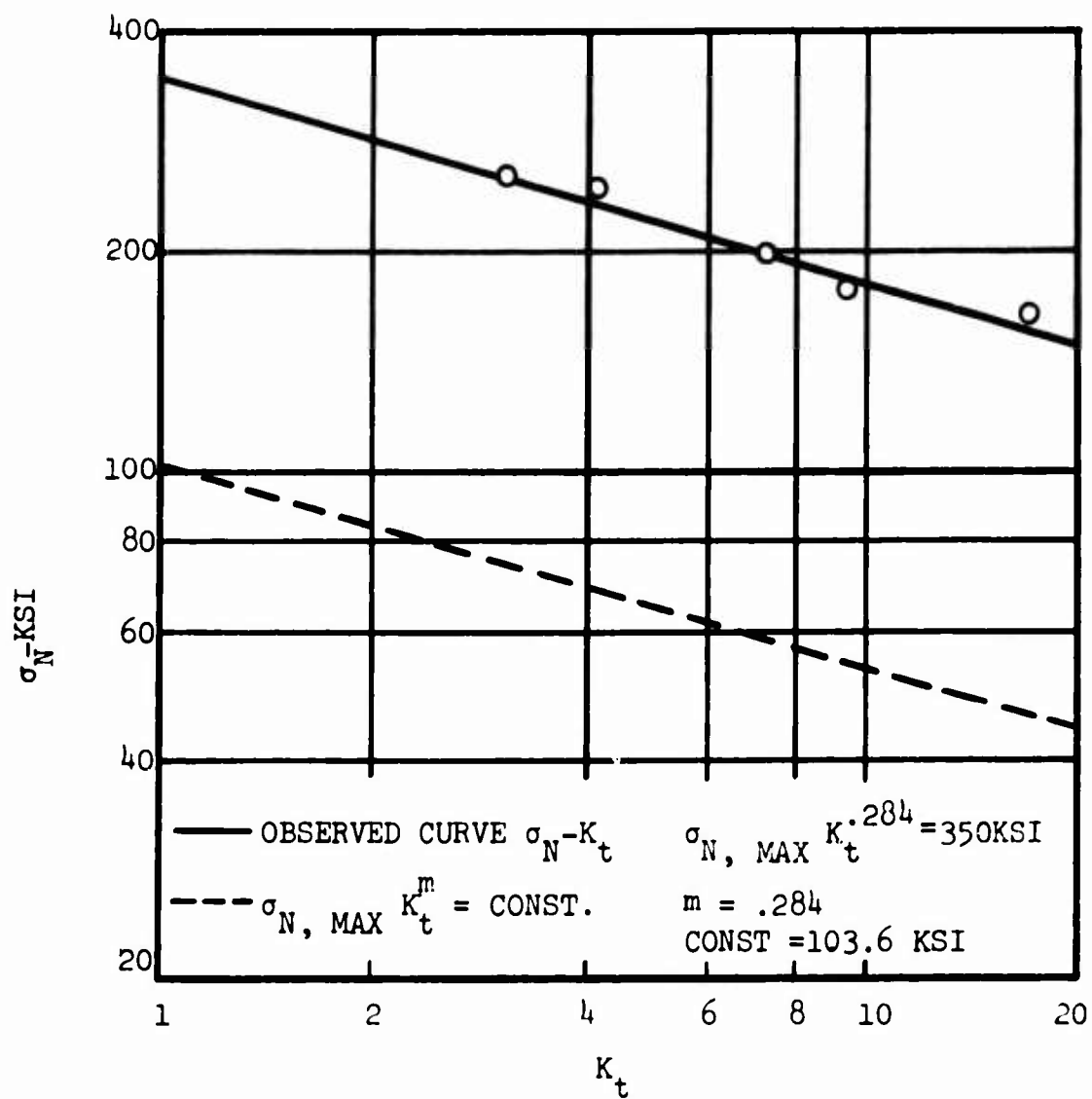
FIG. 2 OBSERVED σ_N-K_t CURVE AND $\sigma_{N,MAX}$-K_t^{m} TESTING CURVE FOR D6AC

26
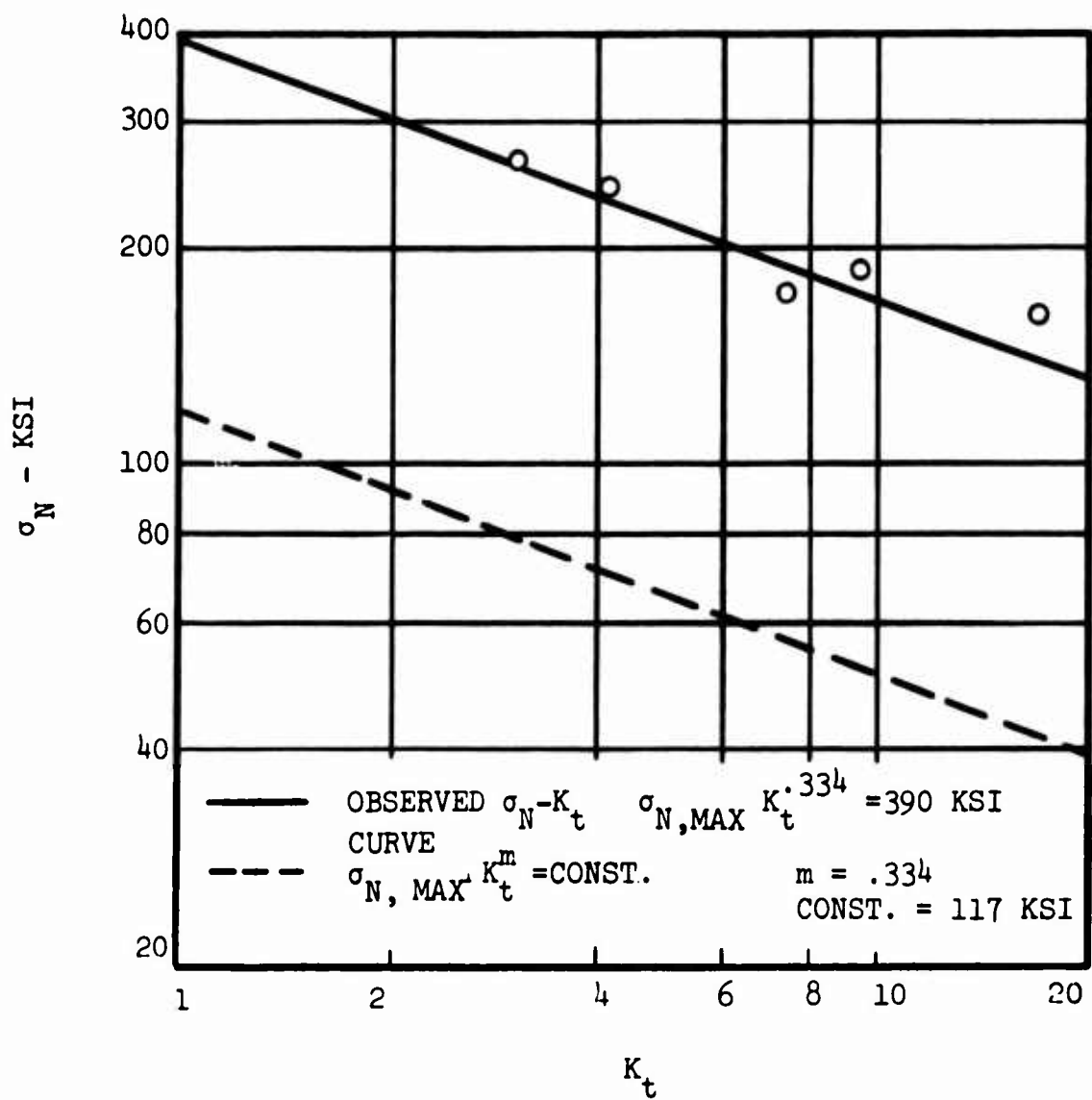
FIG. 3 OBSERVED σ_N - K_t CURVE AND $\sigma_{N,MAX}$-K_t^m TESTING
CURVE FOR HP9-4-25
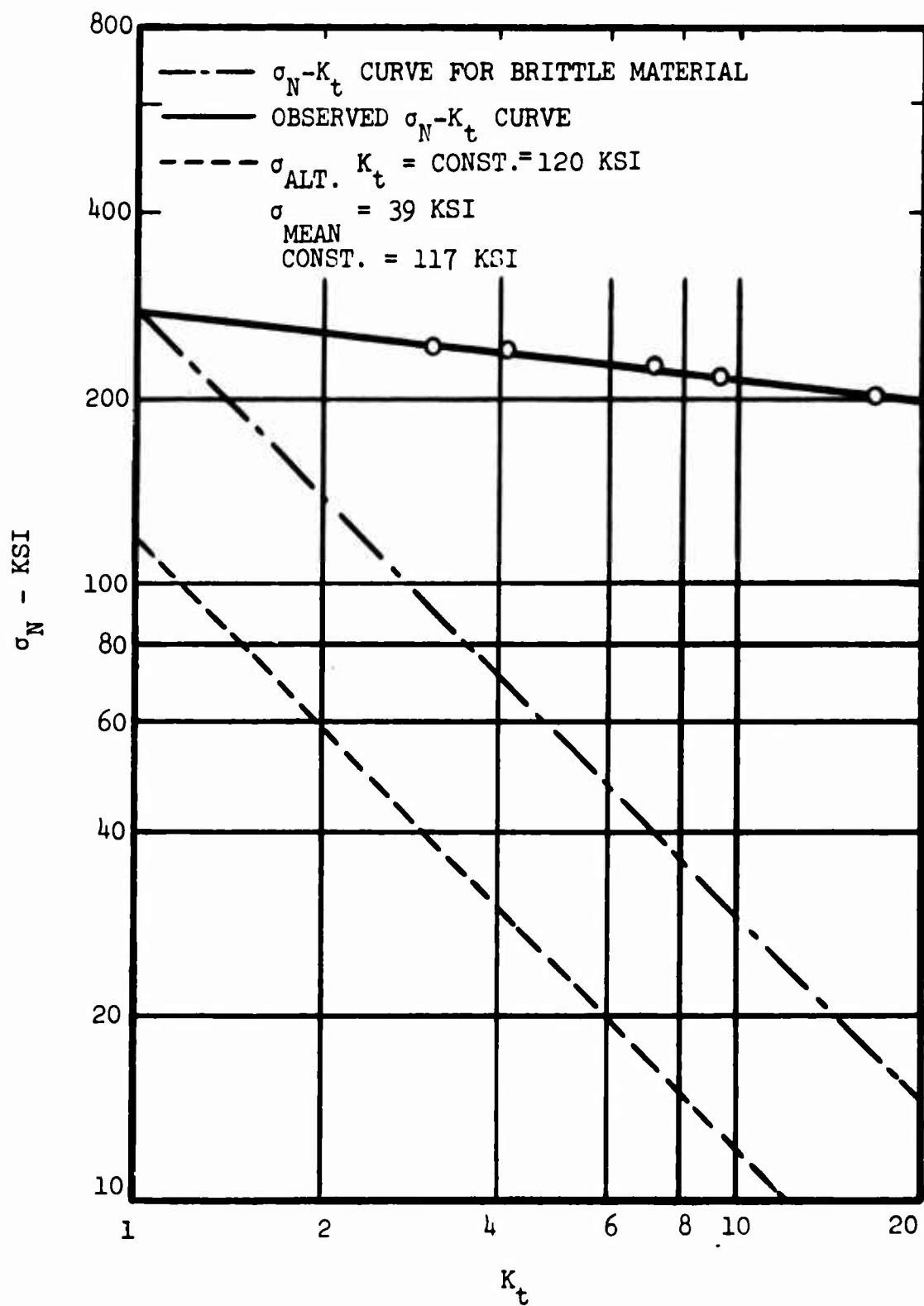
FIG. 4 OBSERVED σ_N - K_t CURVE AND $\sigma_{ALT.}$ - K_t TESTING
CURVE FOR AISI 301 STAINLESS STEEL. (51% COLD
REDUCED)

28
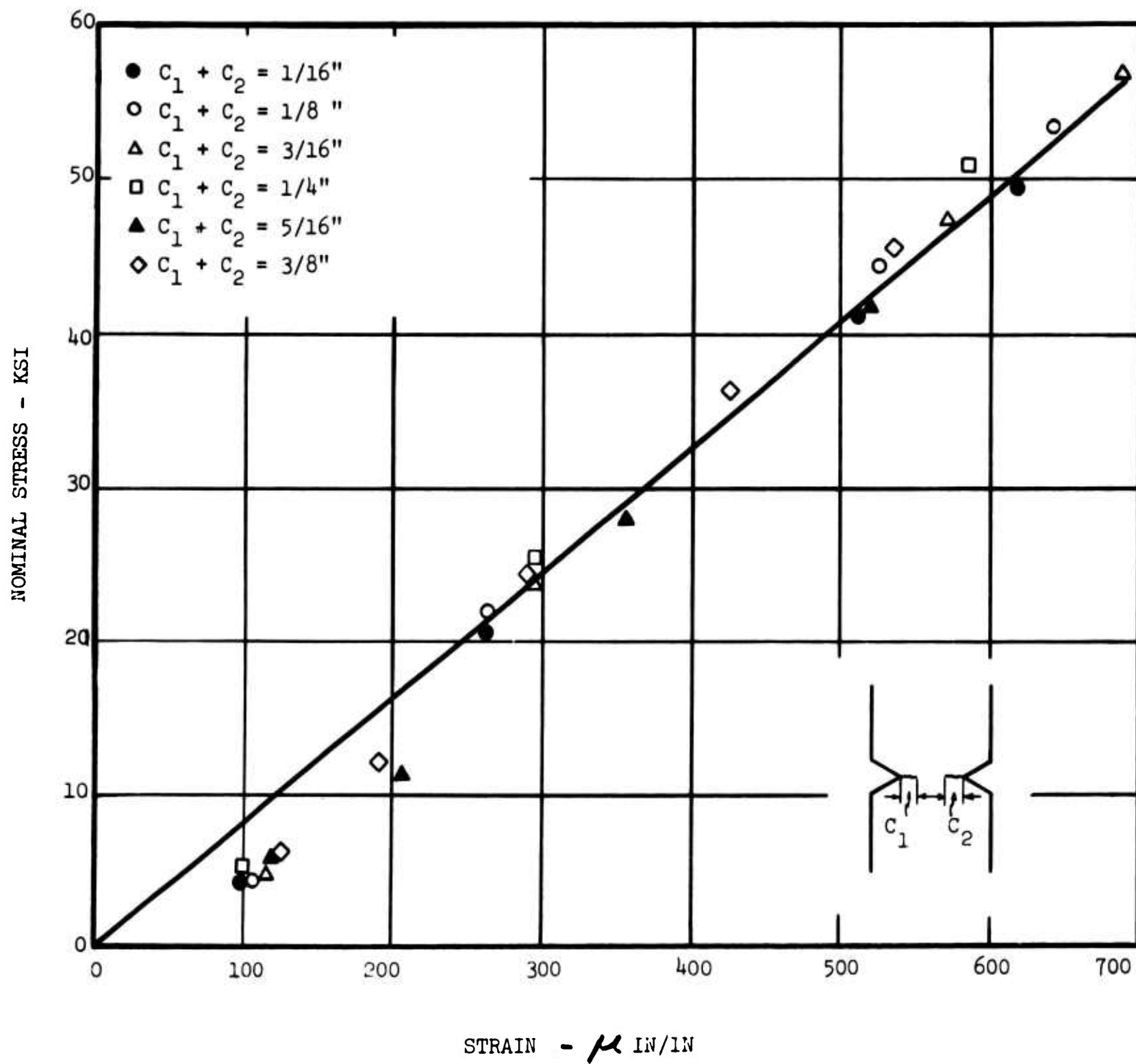
FIG. 5 CALIBRATION CURVES FOR OBTAINING NOMINAL STRESS IN THE SPECIMEN DURING
FATIGUE TESTING (PH-15-7Mo - RH-1050)
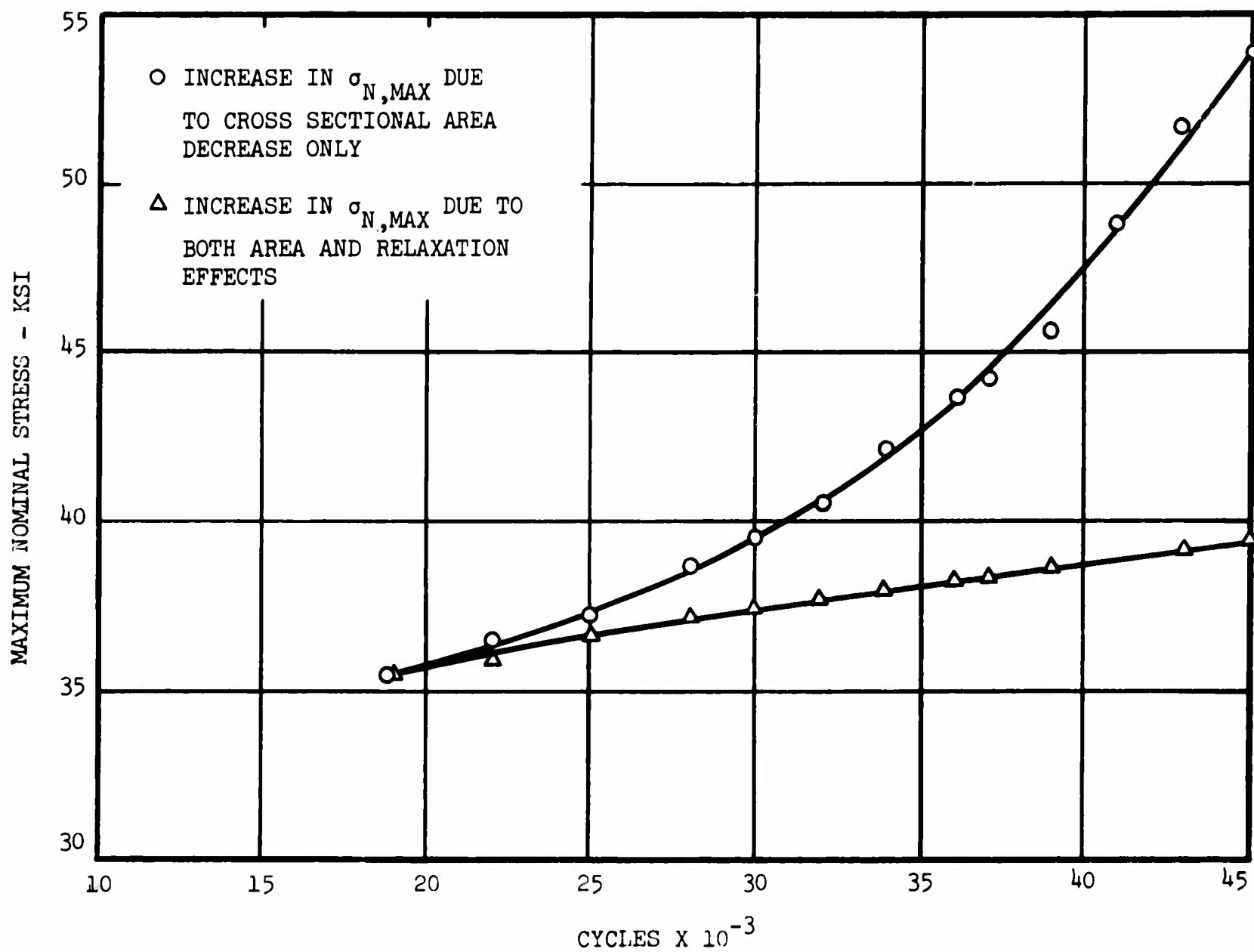
FIG. 6   CHANGE IN THE MAXIMUM NET SECTION STRESS DURING THE FATIGUE TESTING OF
PH-15-7Mo (RH-1050)

30
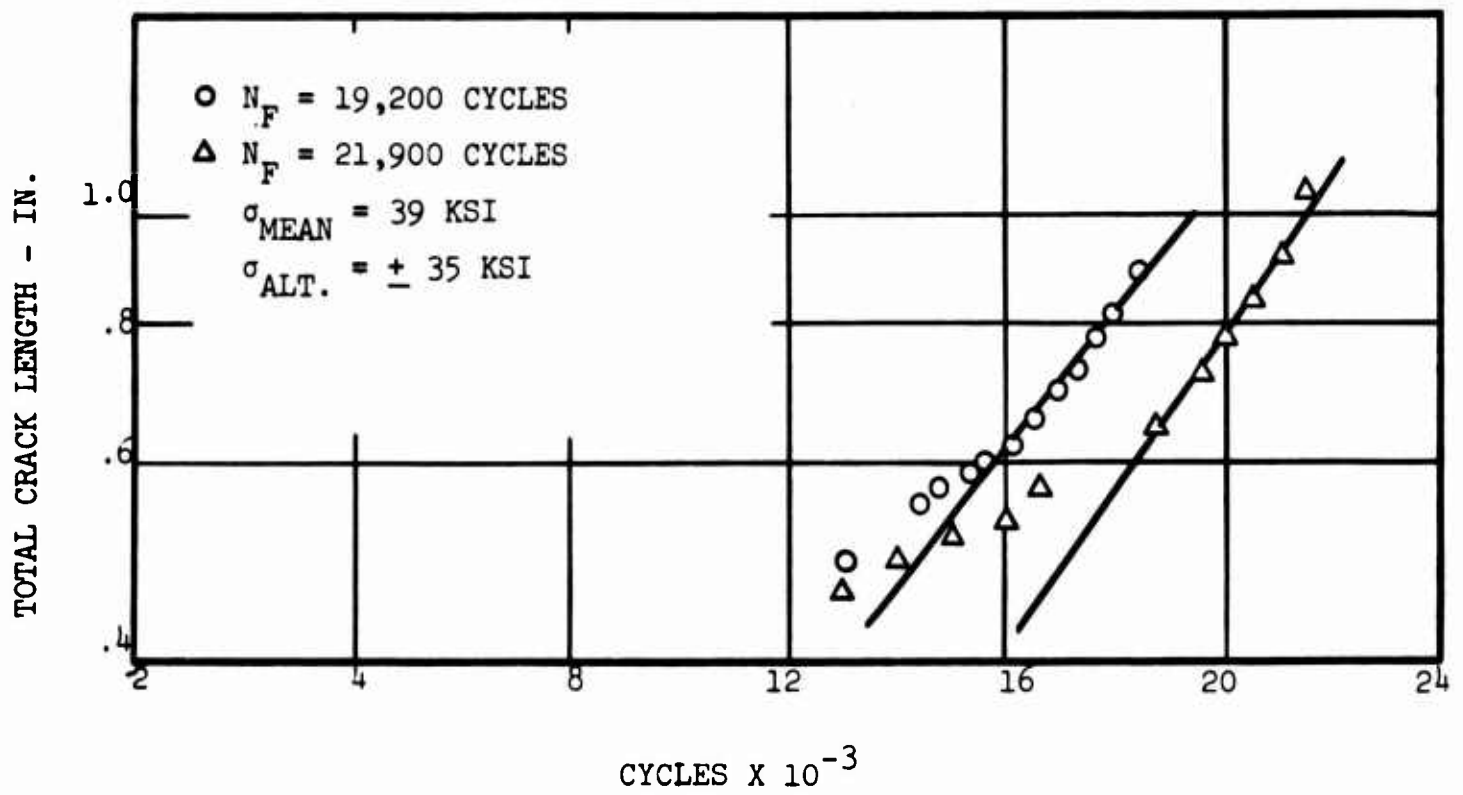
FIG. 7 CRACK LENGTH VS NUMBER OF CYCLES FOR K_t = 3.1 AISI 301
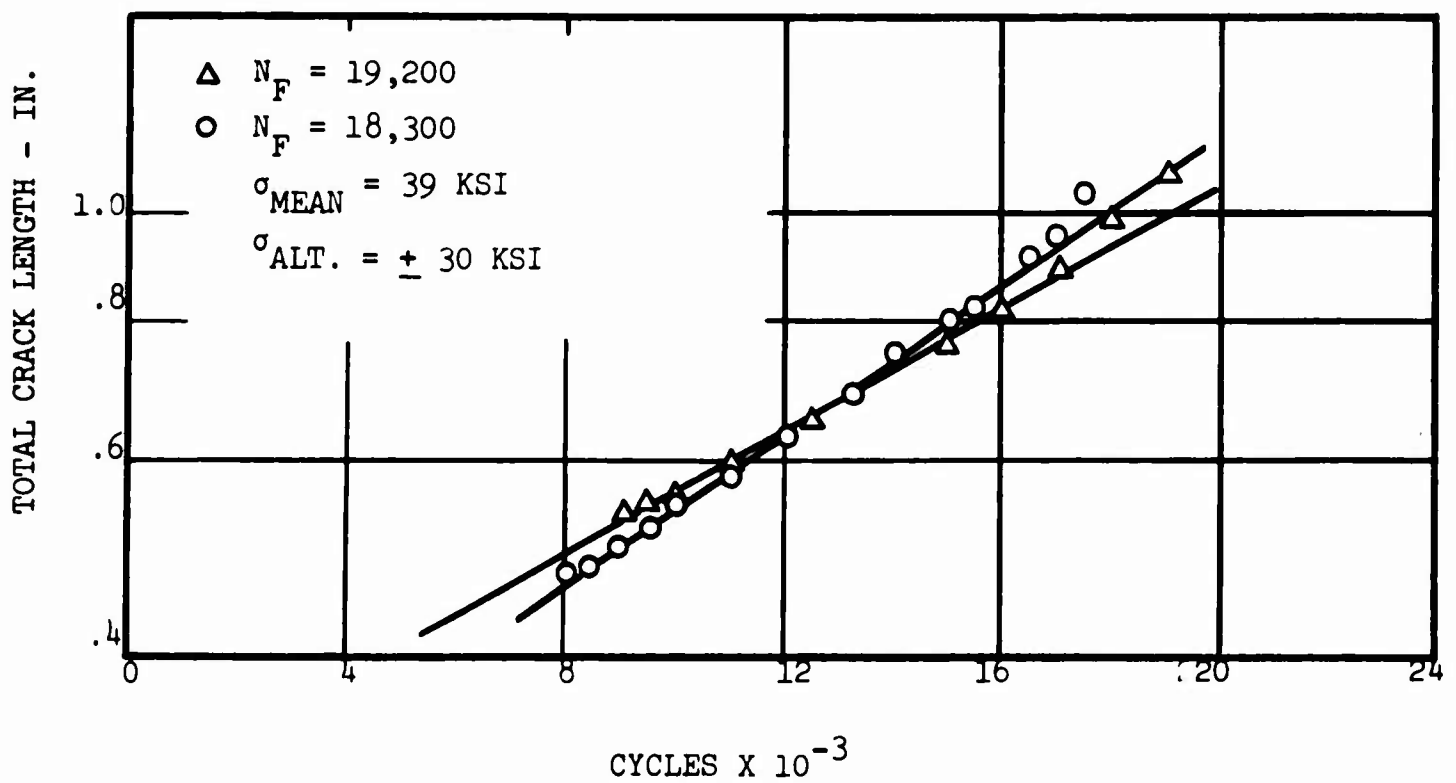
FIG. 8 CRACK LENGTH VS NUMBER OF CYCLES FOR K_t = 4.1 AISI 301

31
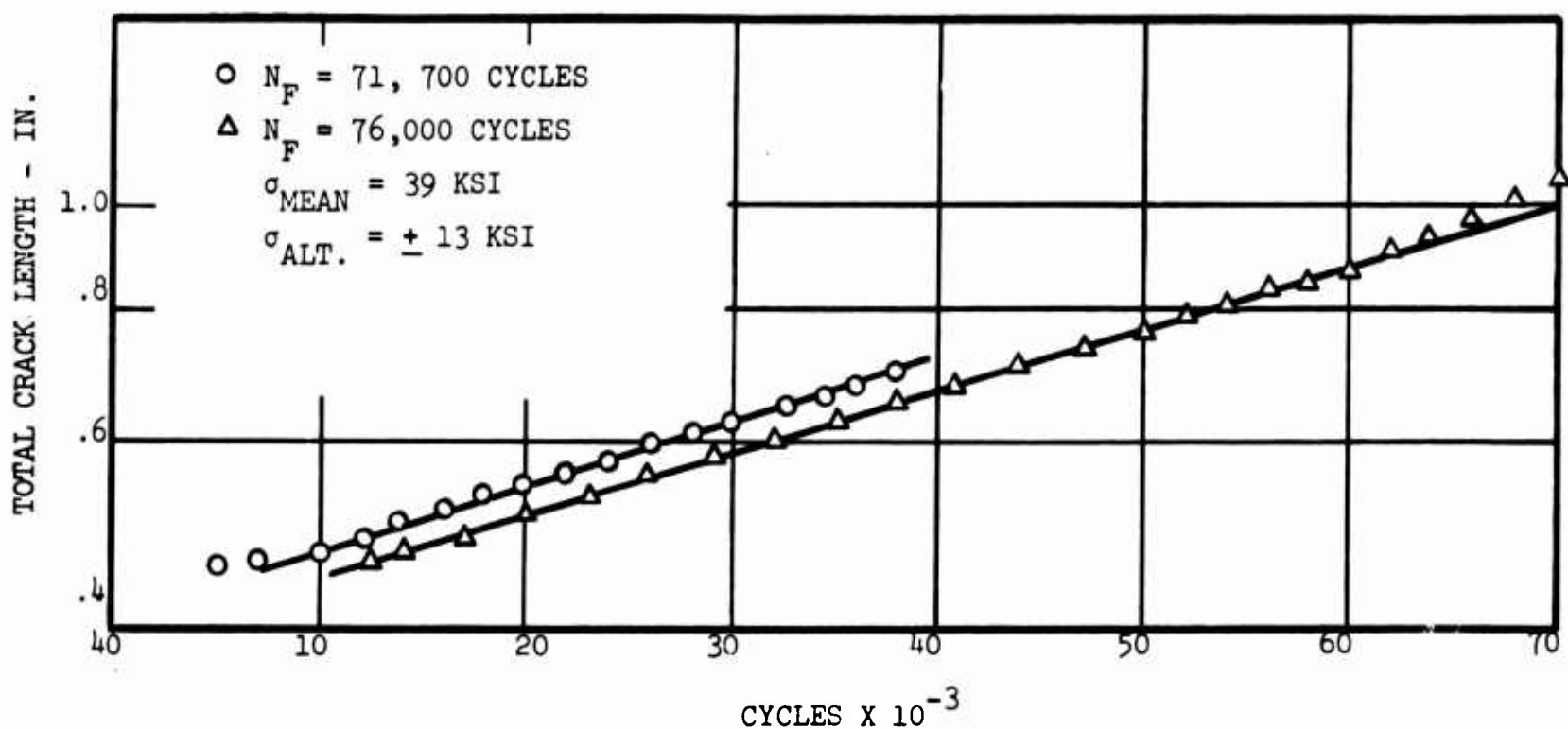
FIG. 9 CRACK LENGTH VS NUMBER OF CYCLES FOR K_t = 9.4 AISI 301
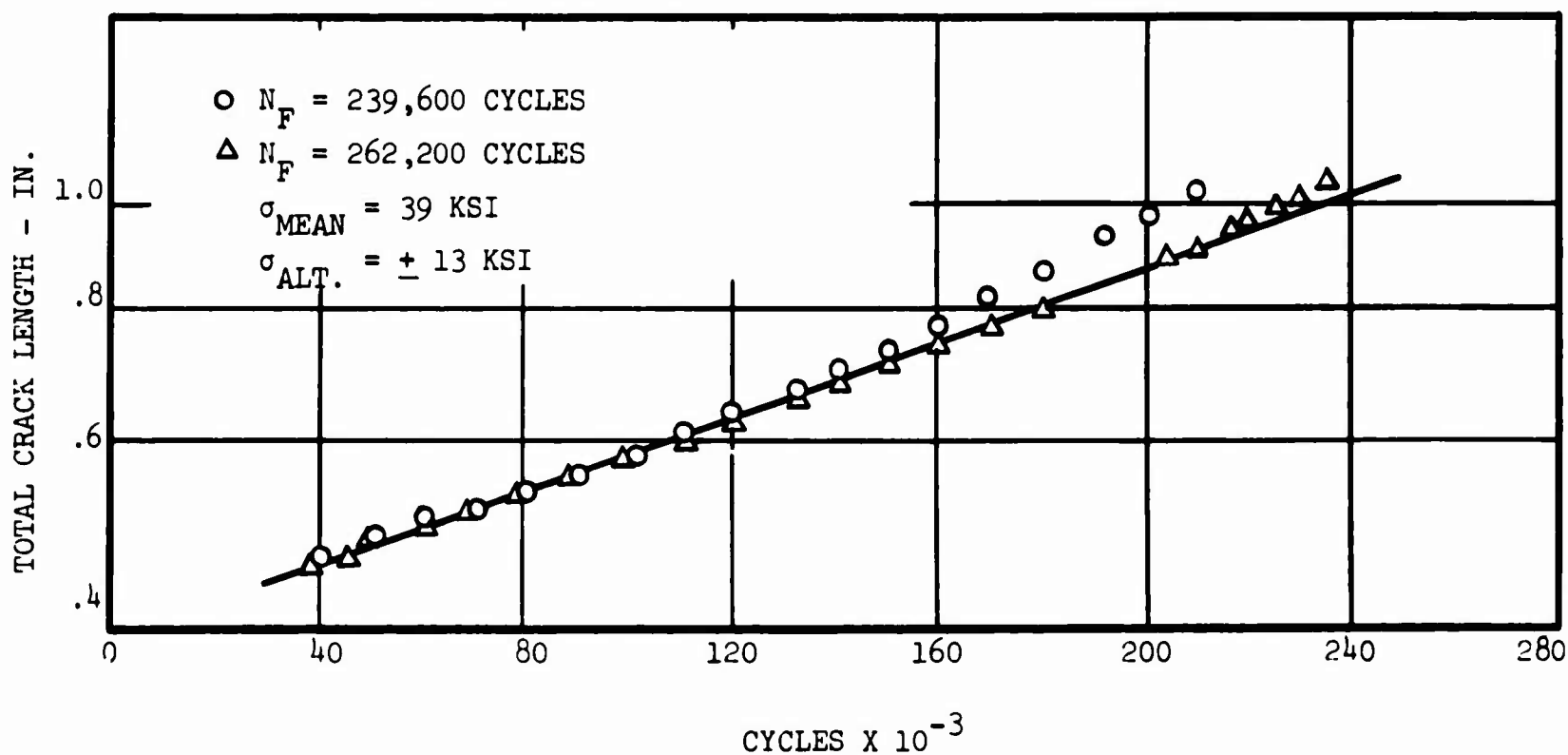
FIG. 10 CRACK LENGTH VS NUMBER OF CYCLES FOR K_t = 17 AISI 301
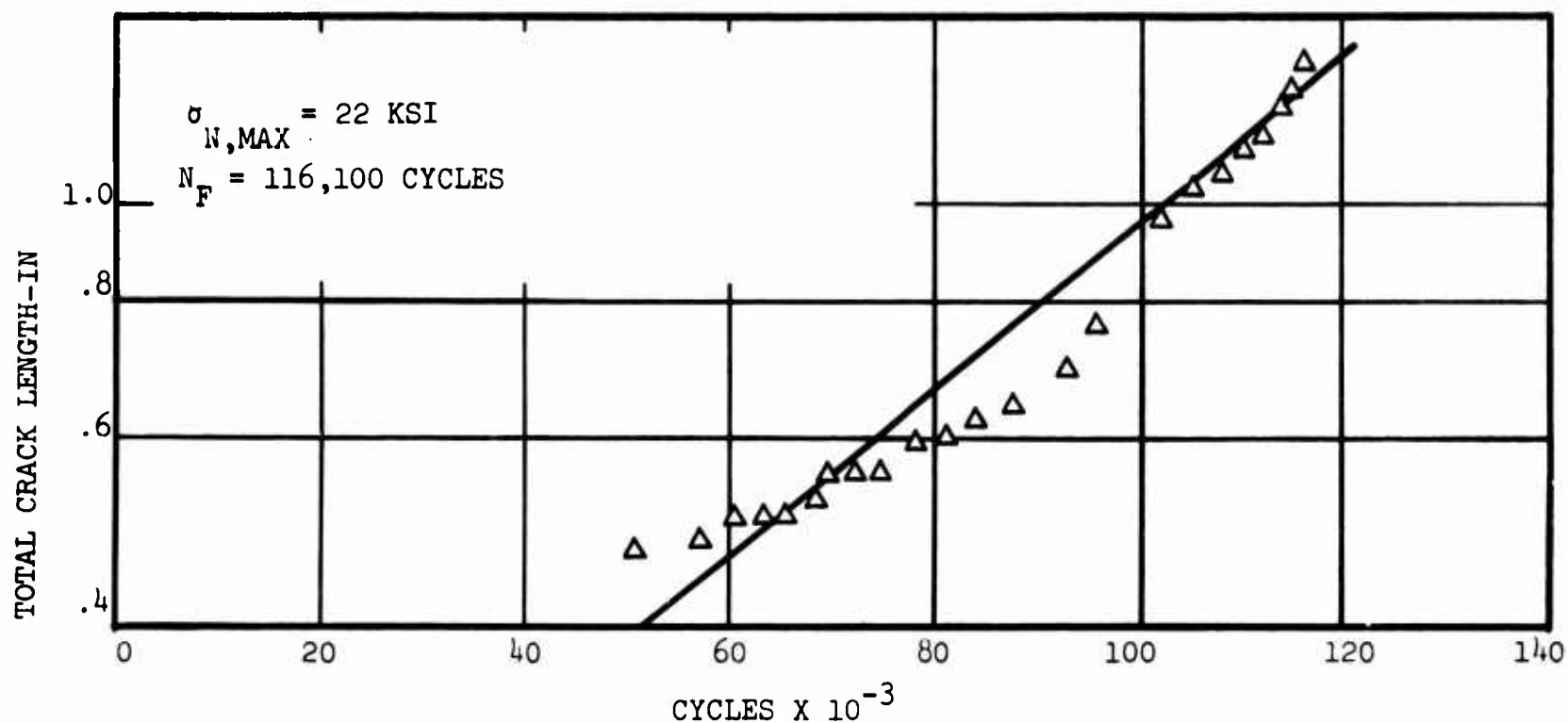
FIG. 11   CRACK LENGTH VS NUMBER OF CYCLES FOR RS-120 (ANNEALED)
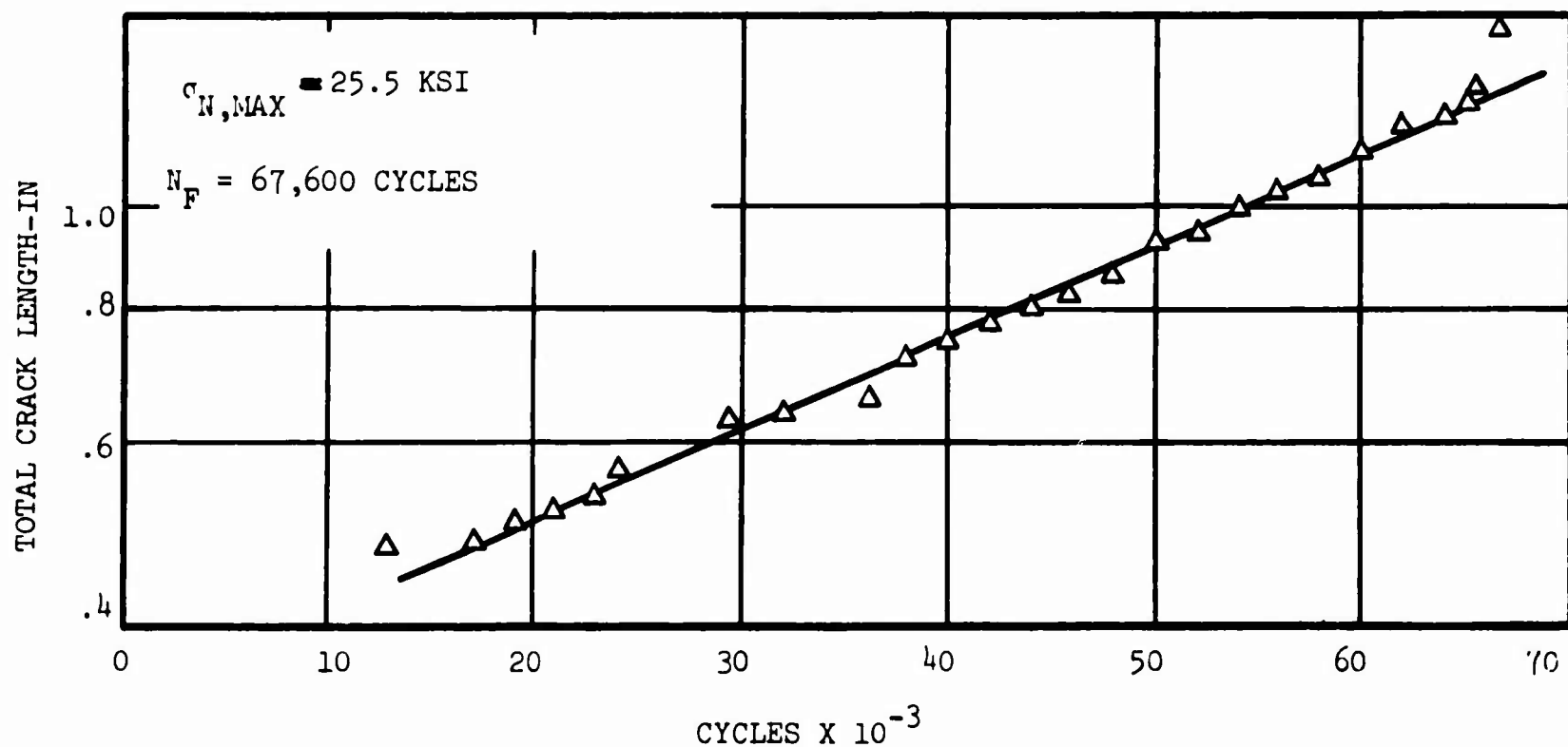
FIG. 12   CRACK LENGTH VS NUMBER OF CYCLES FOR RS-120 (ANNEALED)

33
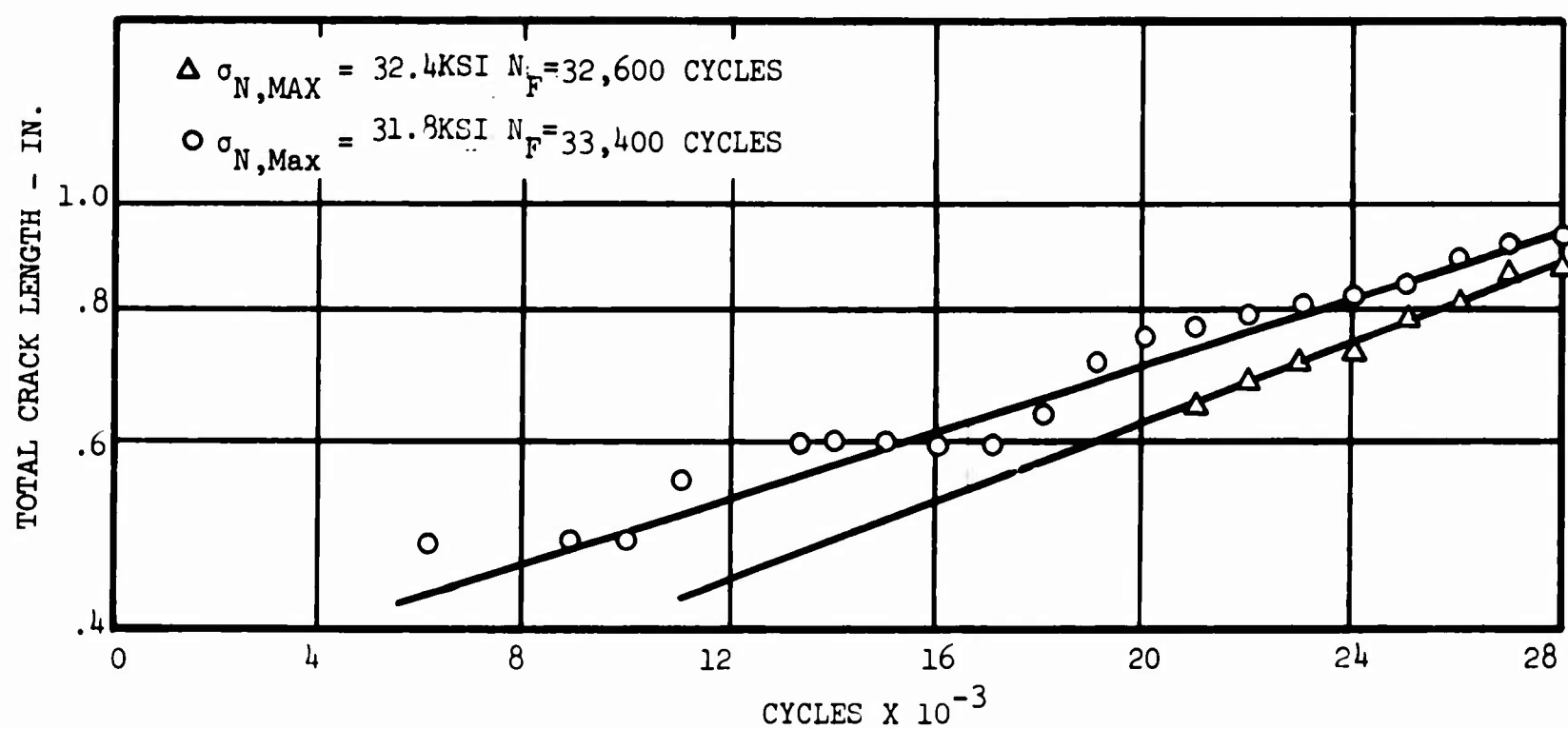
FIG. 13   CRACK LENGTH VS NUMBER OF CYCLES FOR RS-120 (ANNEALED)
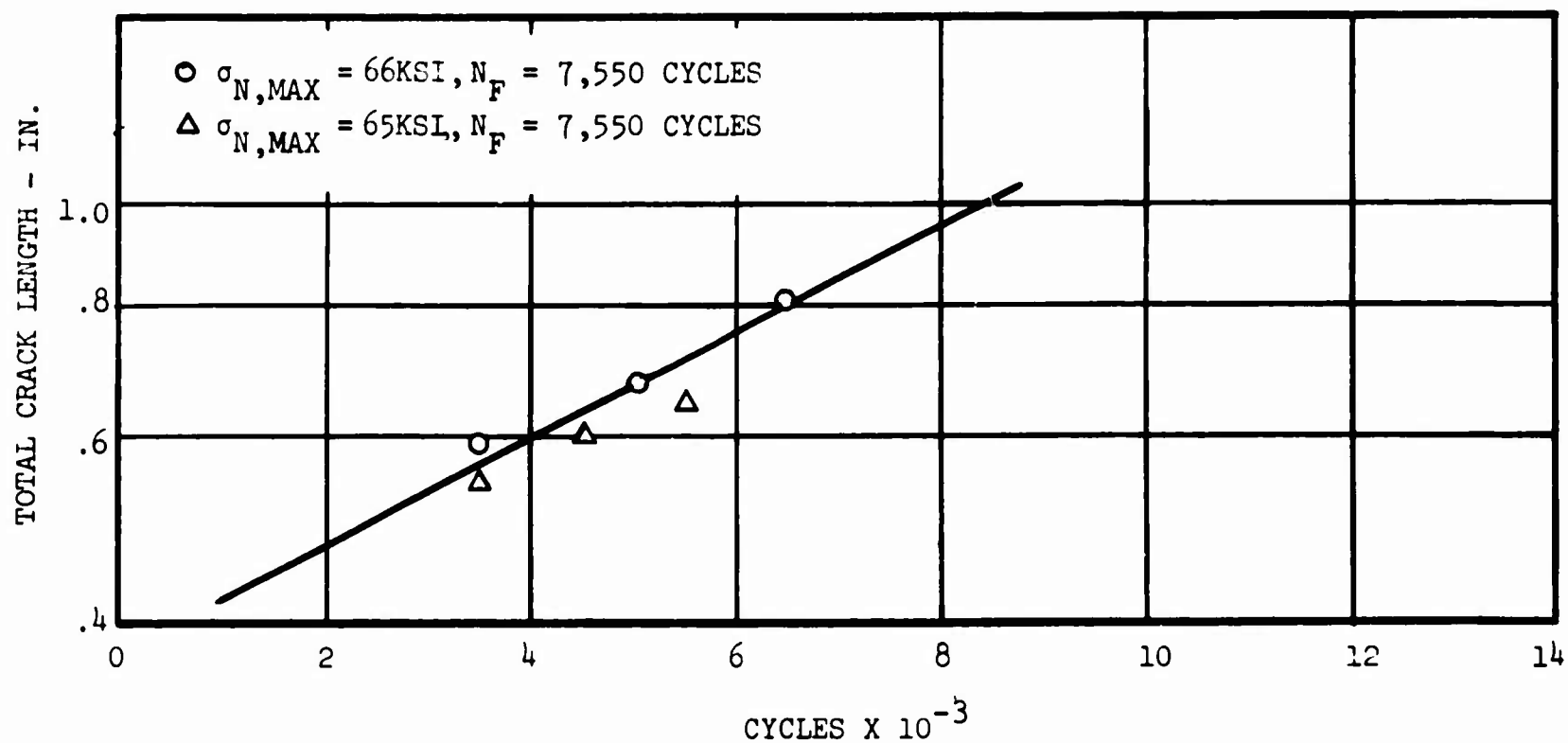
FIG. 14   CRACK LENGTH VS NUMBER OF CYCLES FOR RS-120 (ANNEALED)

34

$\sigma_{N,MAX}$ = 34.6 KSI

N_F = 56,600 CYCLES

FIG. 15 CRACK LENGTH VS NUMBER OF CYCLES FOR PH-15-7Mo (CH 900)

$\sigma_{N,MAX}$ = 28.0 KSI

N_F = 106,200 CYCLES
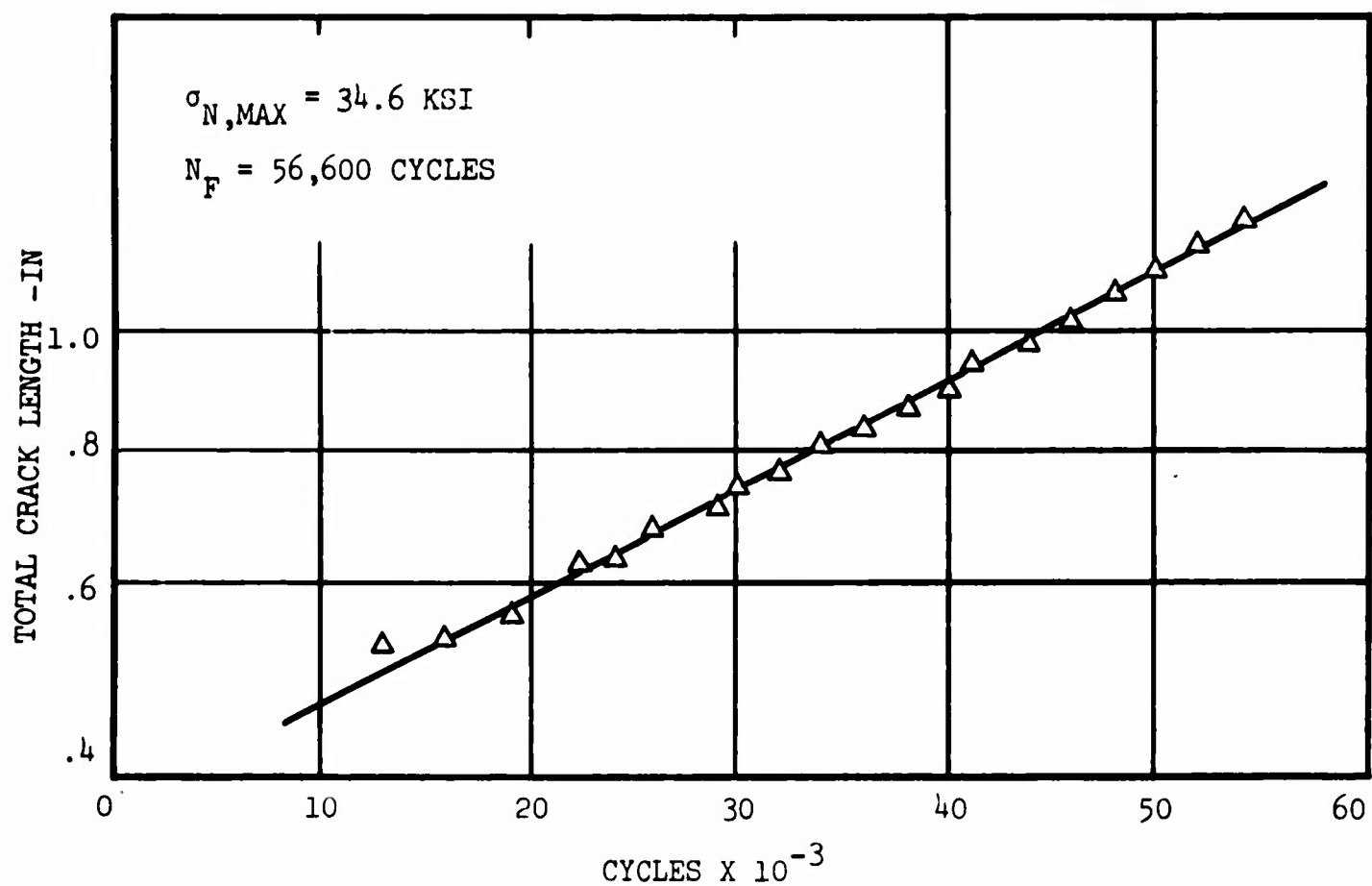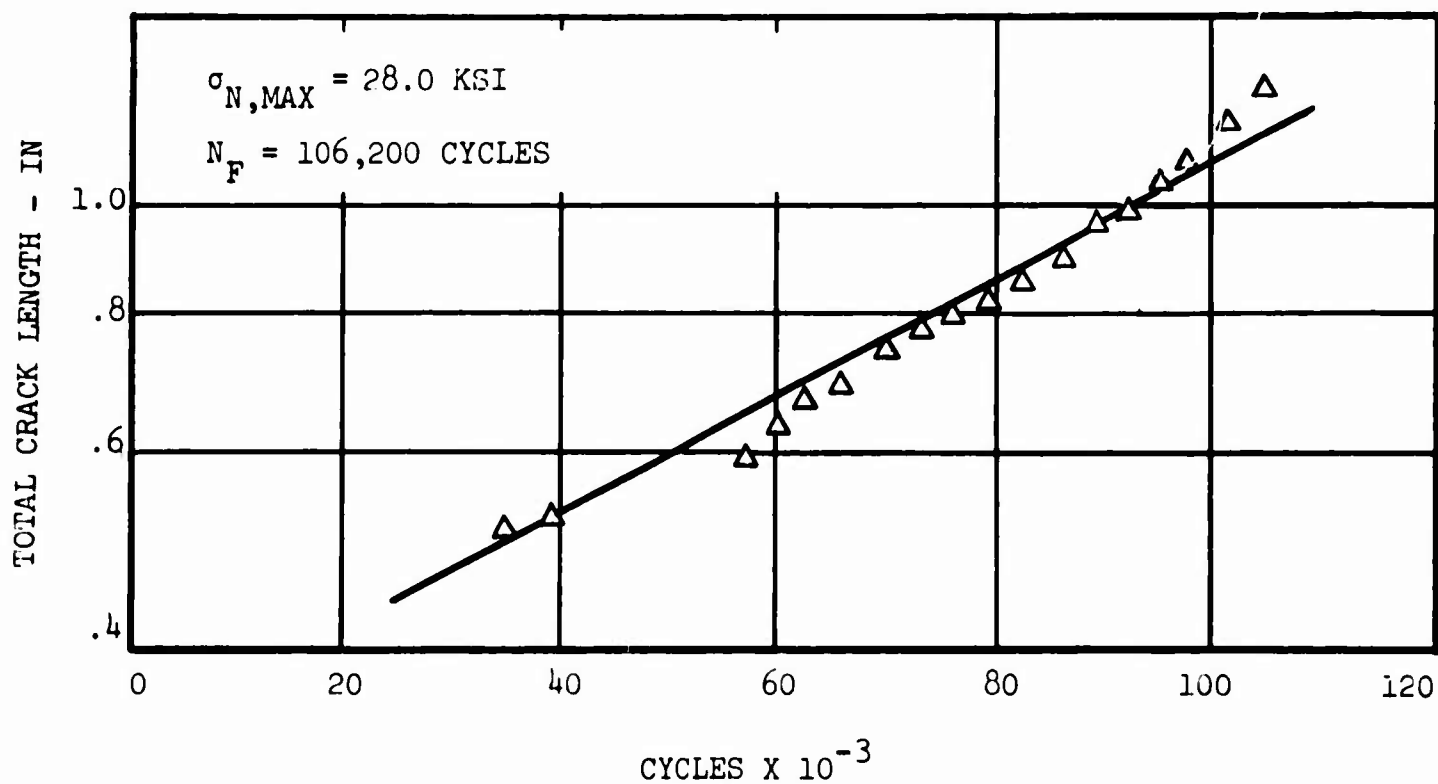
FIG. 16 CRACK LENGTH VS NUMBER OF CYCLES FOR PH-15-7Mo (CH-900)
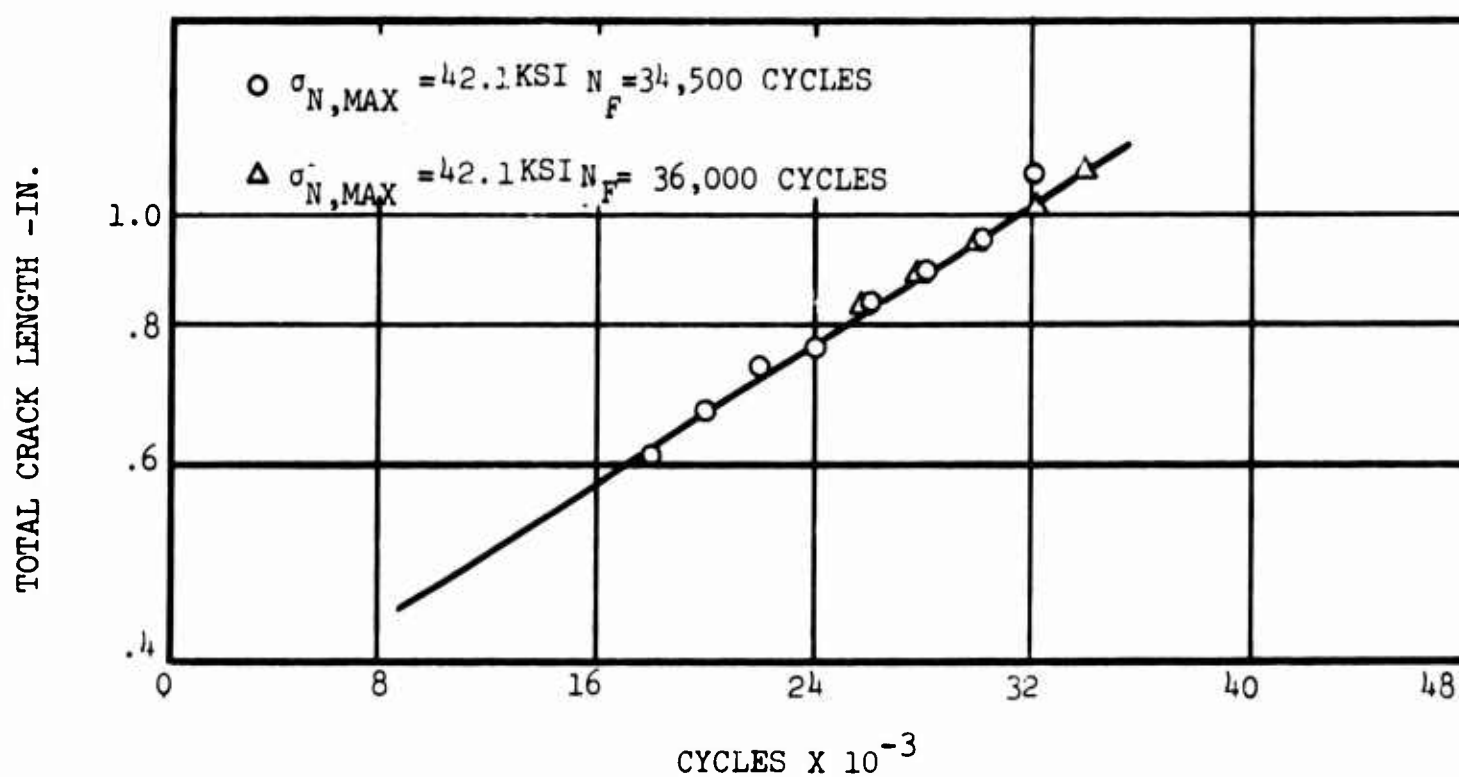
FIG. 17   CRACK LENGTH VS NUMBER OF CYCLES FOR PH-15-7Mo (CH-900)
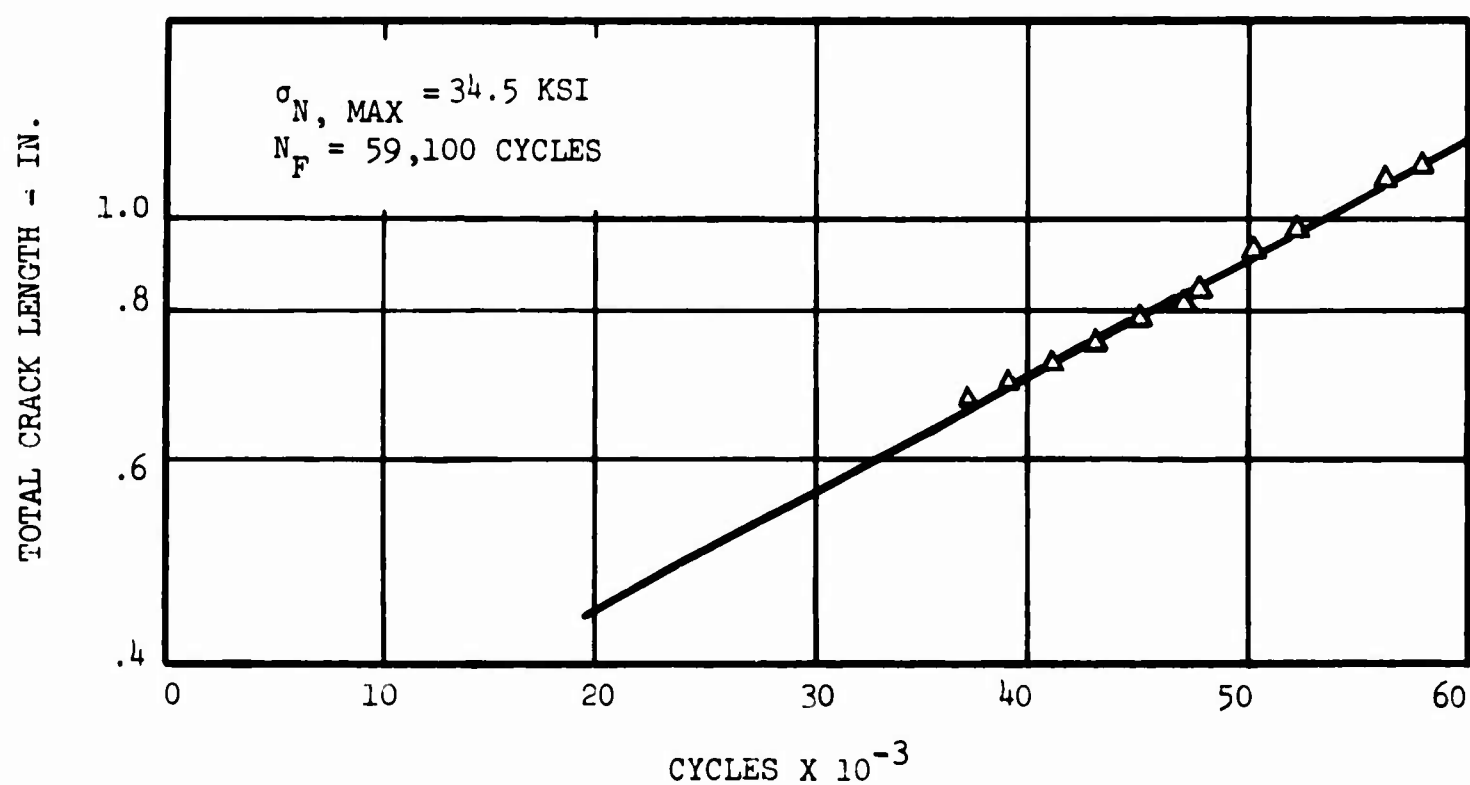
FIG. 18   CRACK LENGTH VS NUMBER OF CYCLES FOR PH-15-7Mo (RH-1050)

36
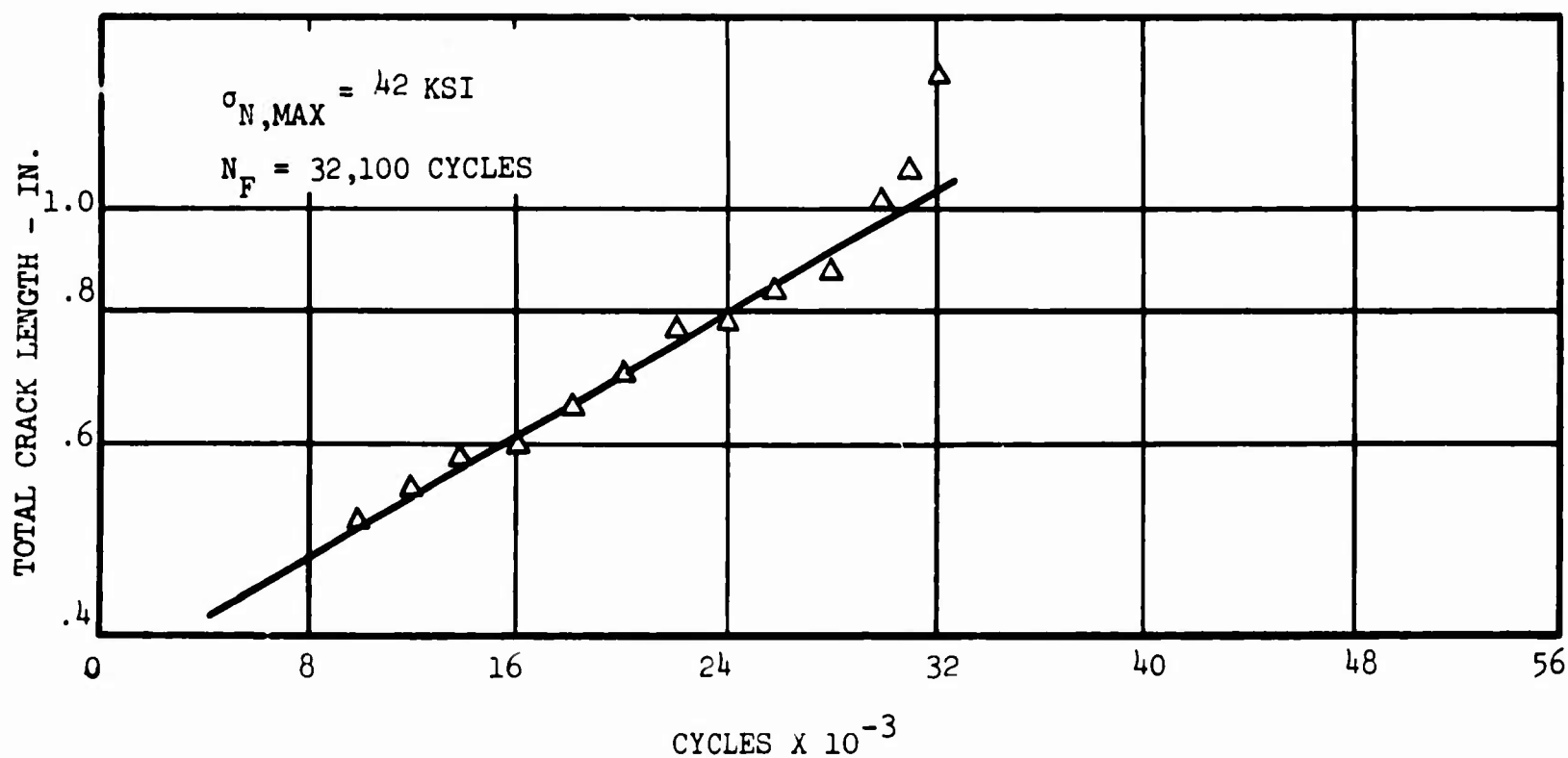
FIG. 19   CRACK LENGTH VS NUMBER OF CYCLES FOR PH-15-7Mo (RH-1050)
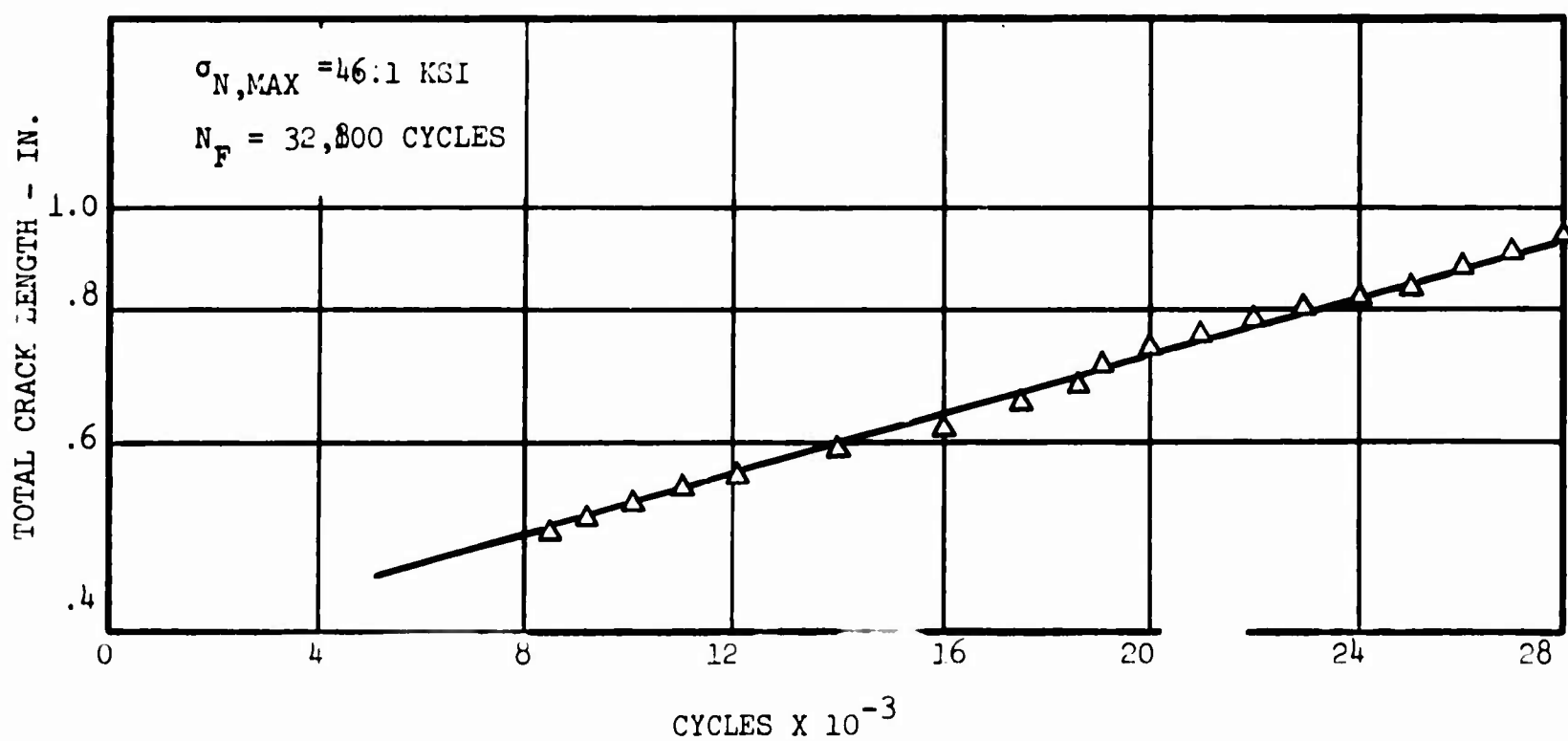
FIG. 20   CRACK LENGTH VS NUMBER OF CYCLES FOR PH-15-7Mo (RH 1050)
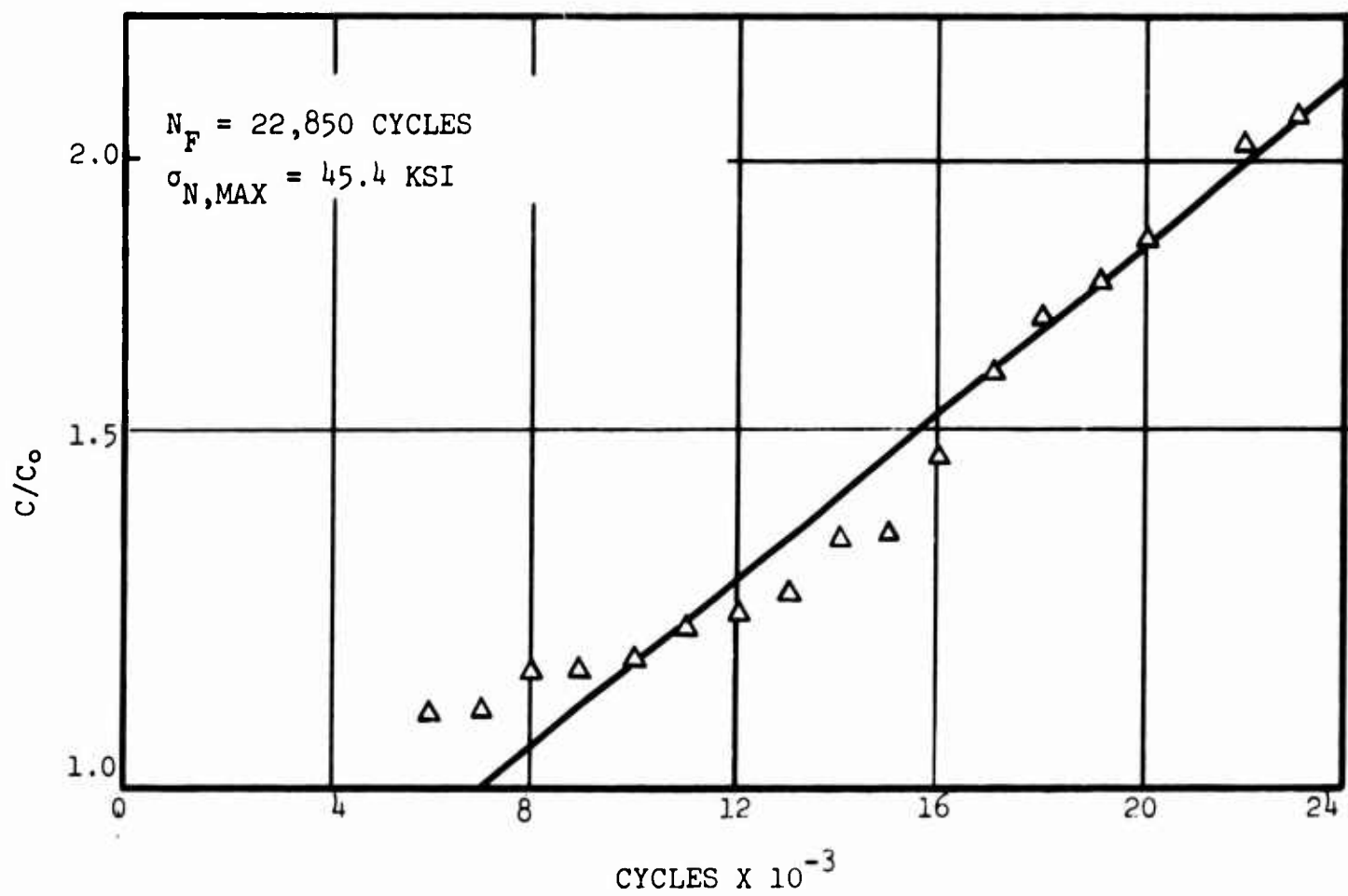
FIG. 21   CRACK LENGTH VERSUS NUMBER OF CYCLES FOR HP9-4-25 K_t= 17
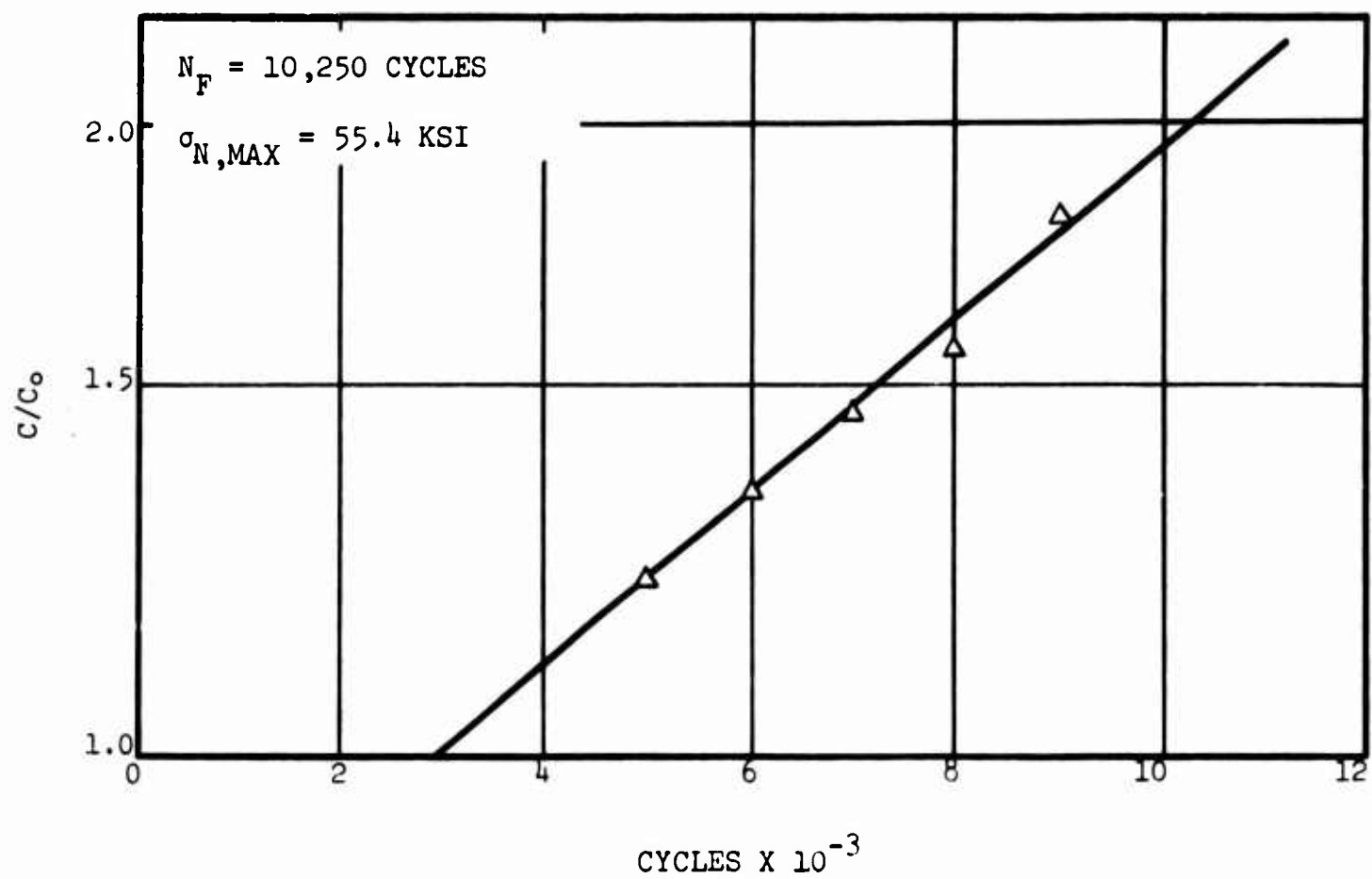
FIG. 22   CRACK LENGTH VERSUS NUMBER OF CYCLES FOR HP9-4-25 K_t= 9.4
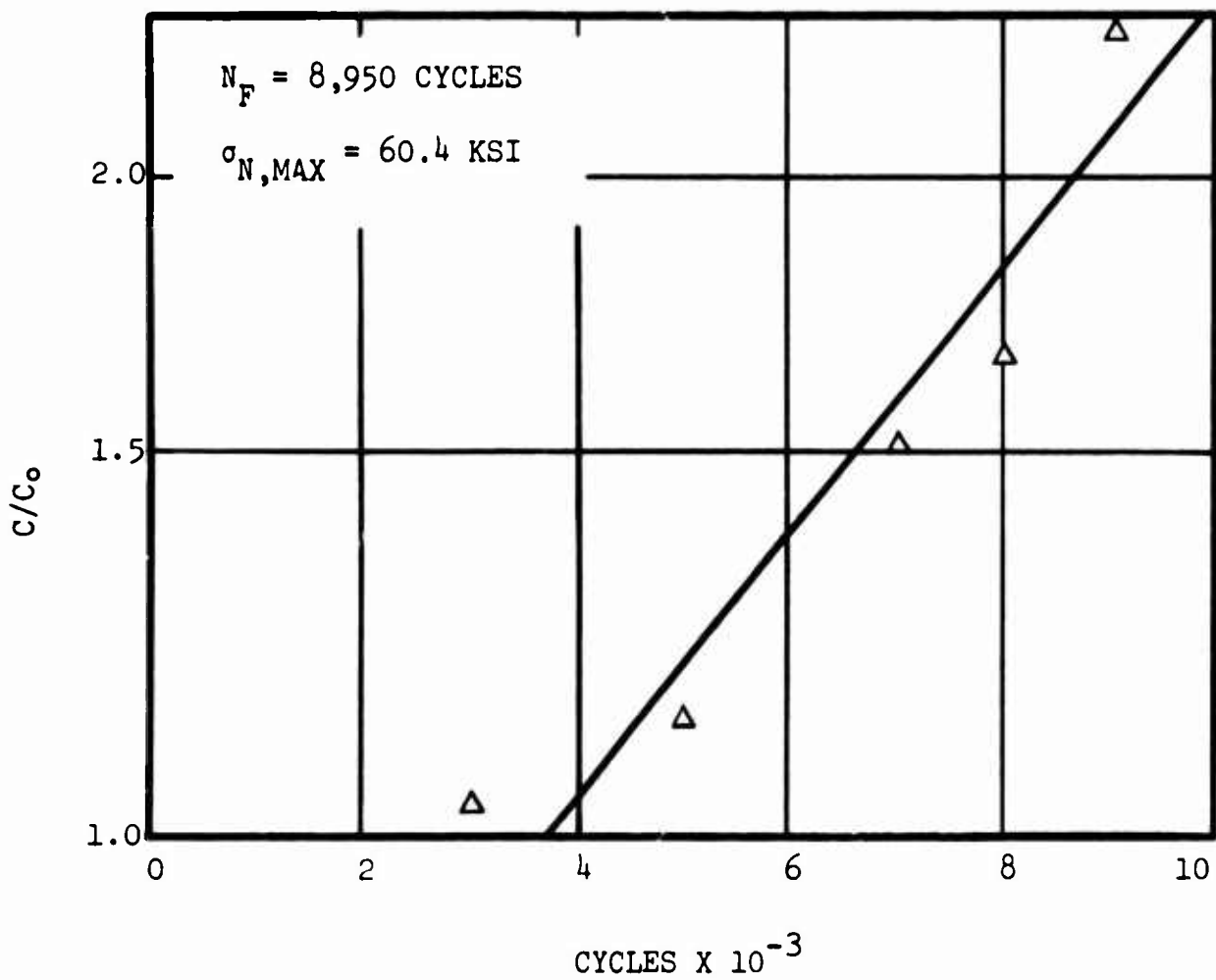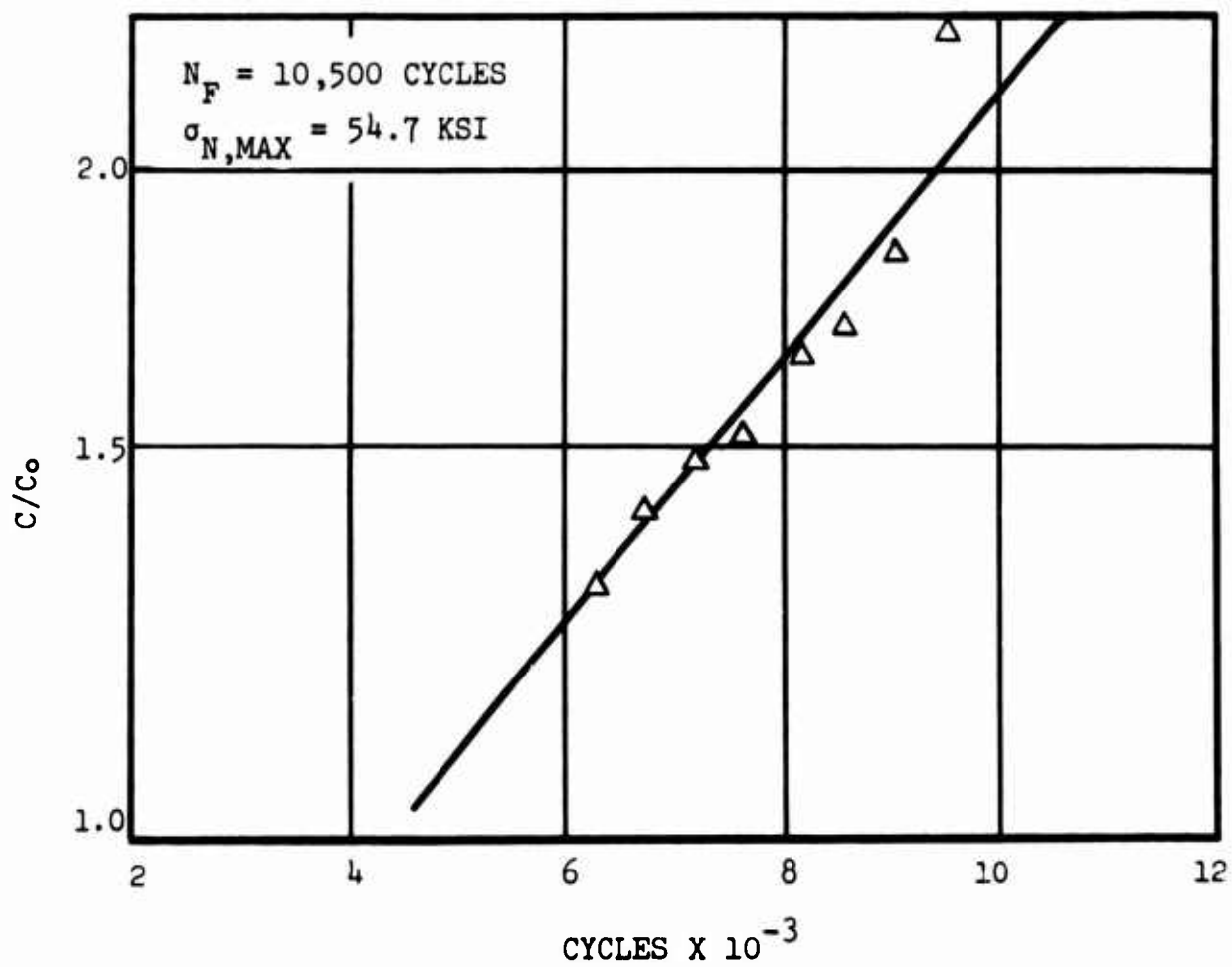
FIG. 23   CRACK LENGTH VERSUS NUMBER OF CYCLES FOR HP9-4-25 K_t = 7.3
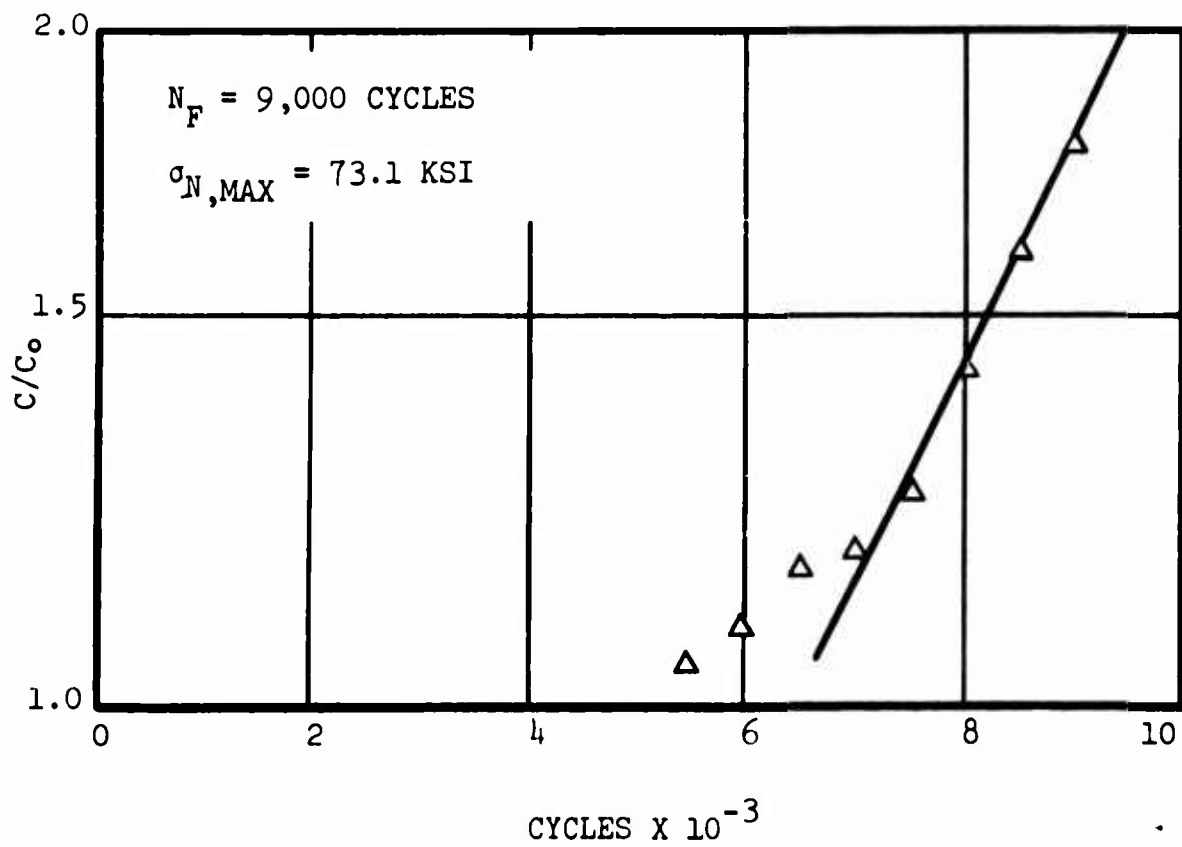
FIG. 24   CRACK LENGTH VERSUS NUMBER OF CYCLES FOR HP9-4-25 K_t = 4.1

39
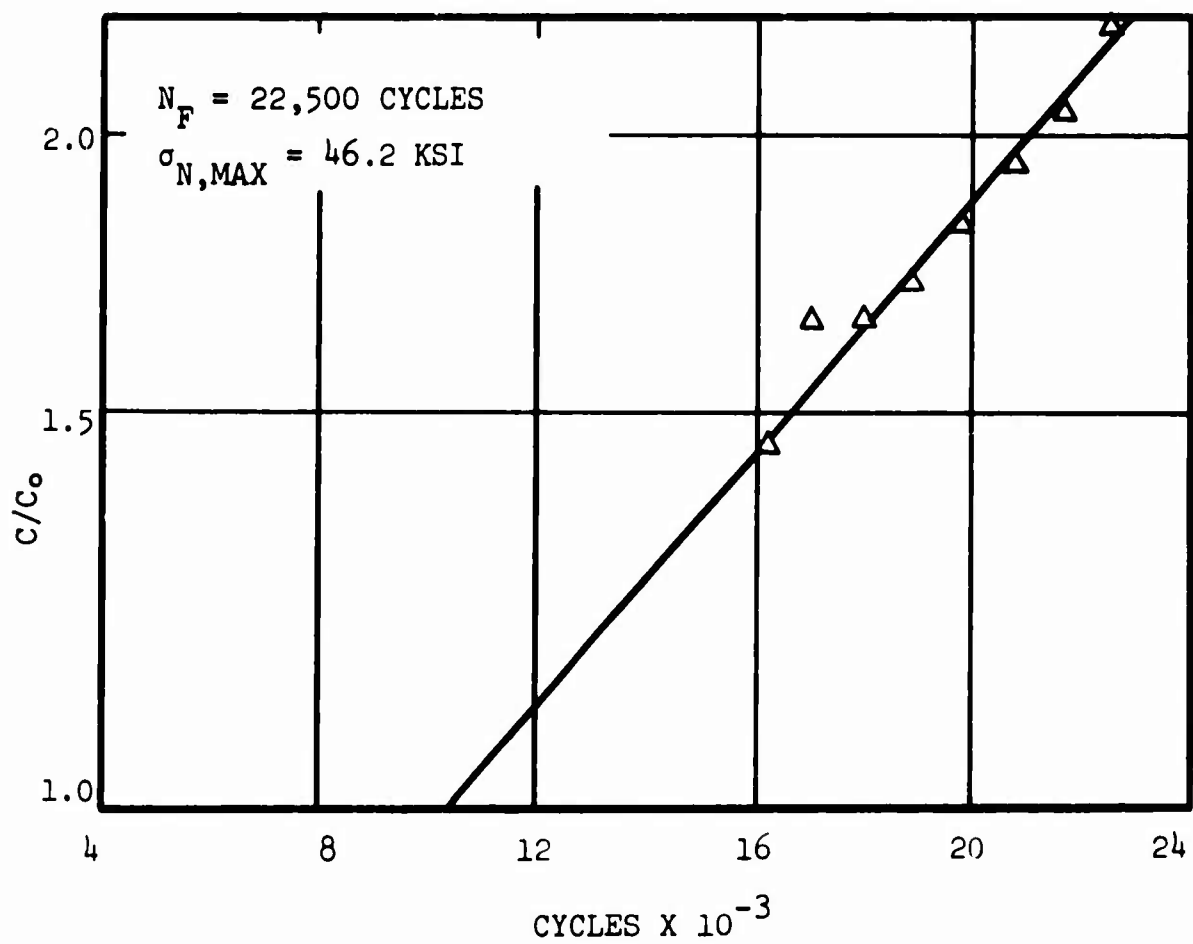
FIG. 25   CRACK LENGTH VERSUS NUMBER OF CYCLES FOR D6AC K_t = 17

FIG. 26   CRACK LENGTH VERSUS NUMBER OF CYCLES FOR D6AC K_t = 9
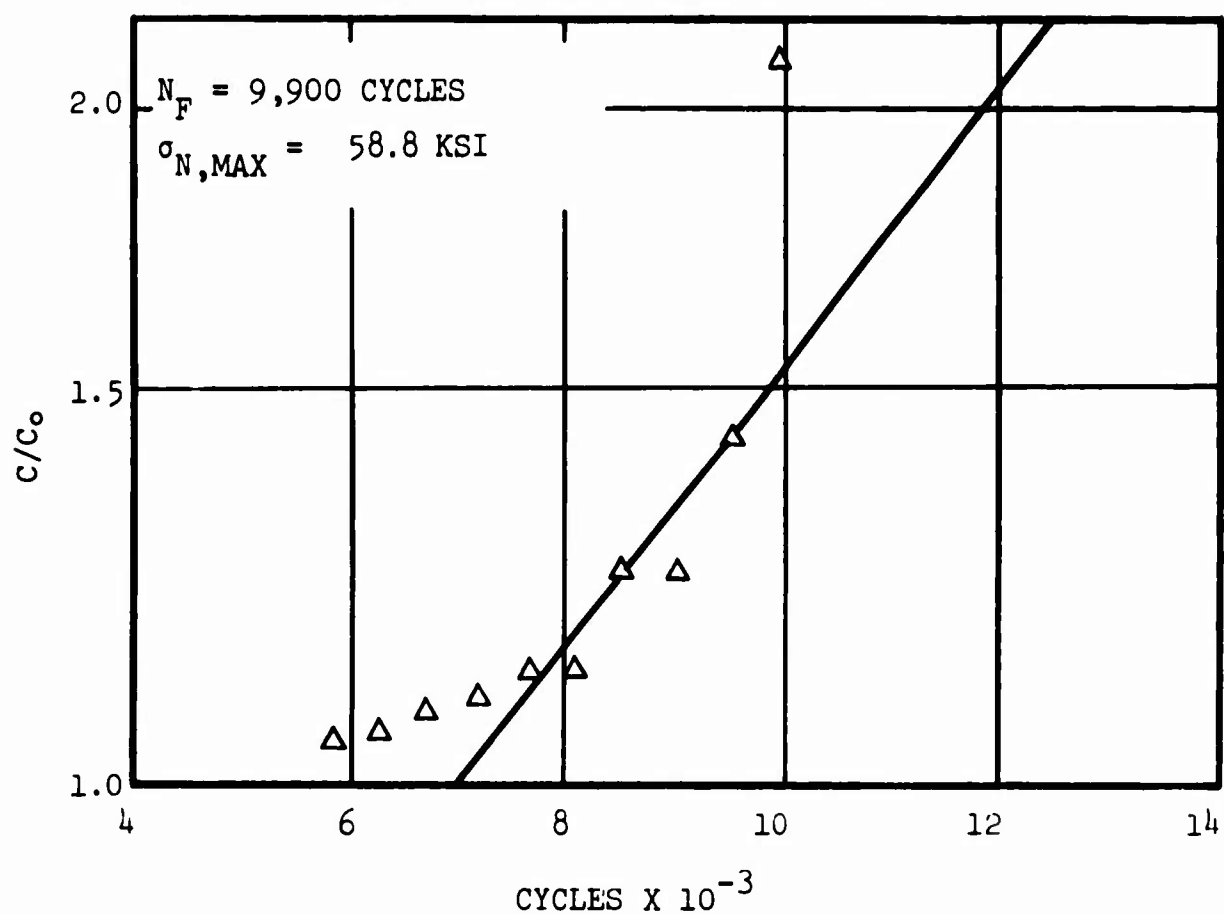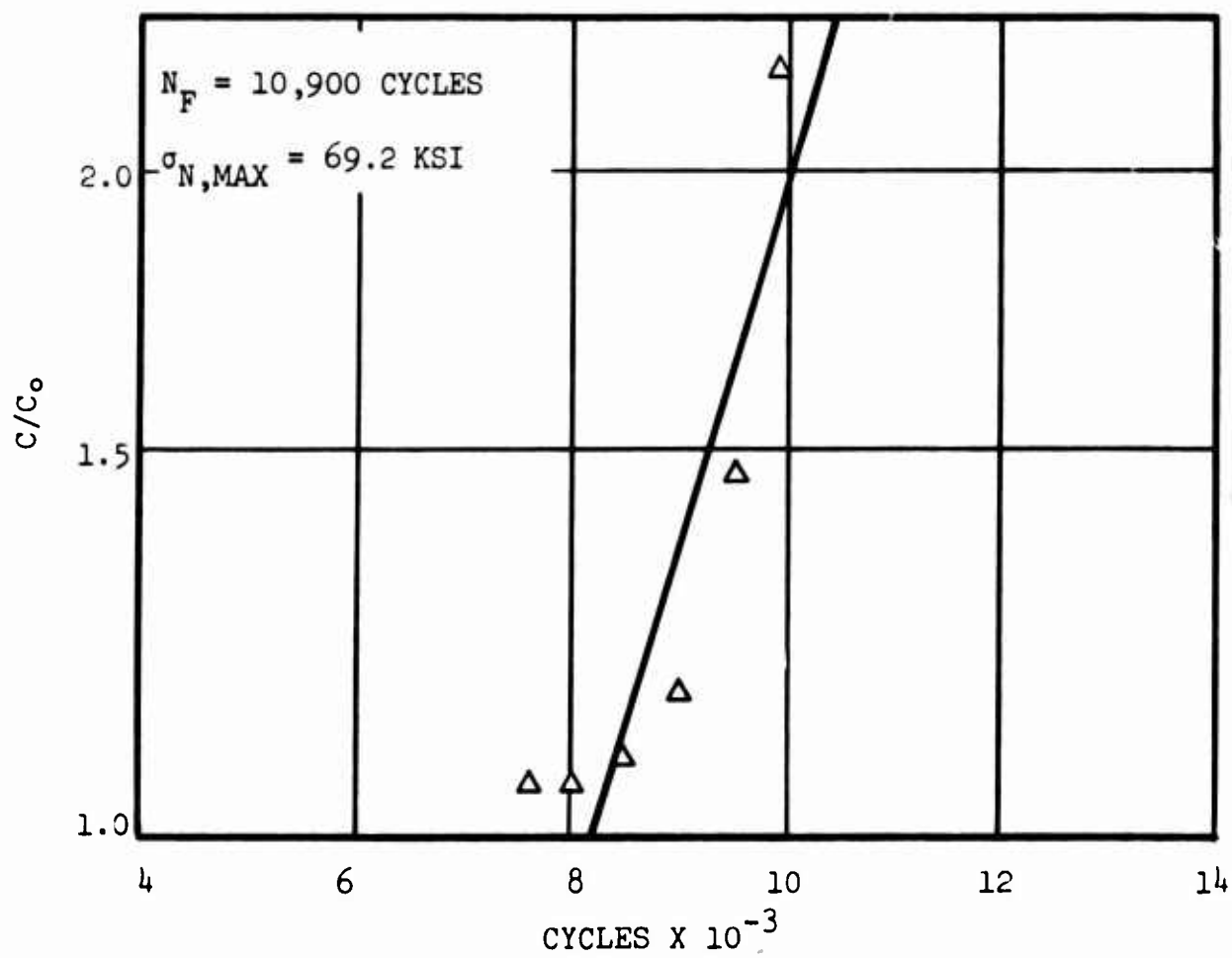
FIG. 27   CRACK LENGTH VERSUS NUMBER OF CYCLES FOR D6AC K_t = 7.3

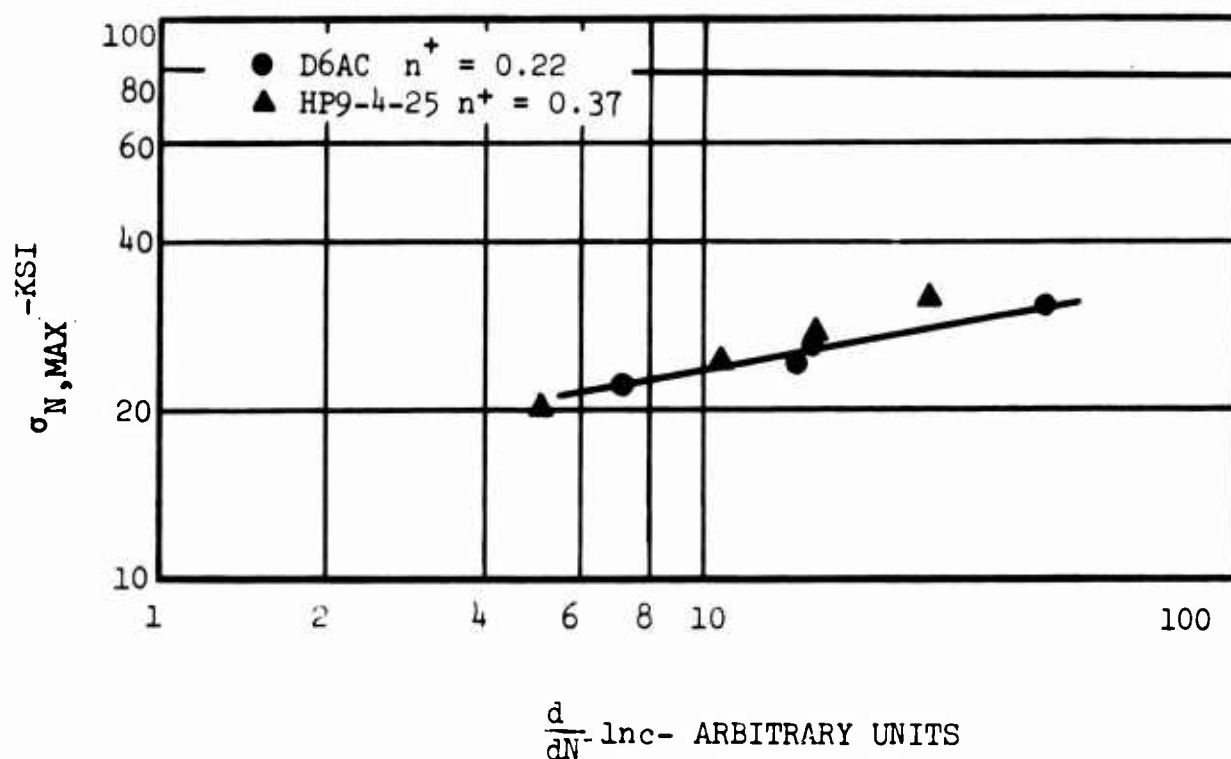FIG. 28   CRACK LENGTH VERSUS NUMBER OF CYCLES FOR D6AC K_t = 4.1.

FIG. 29 $\frac{d}{dN}$Inc VS $\sigma_{N, MAX}$ CURVE FOR THE DETERMINATION OF n^+
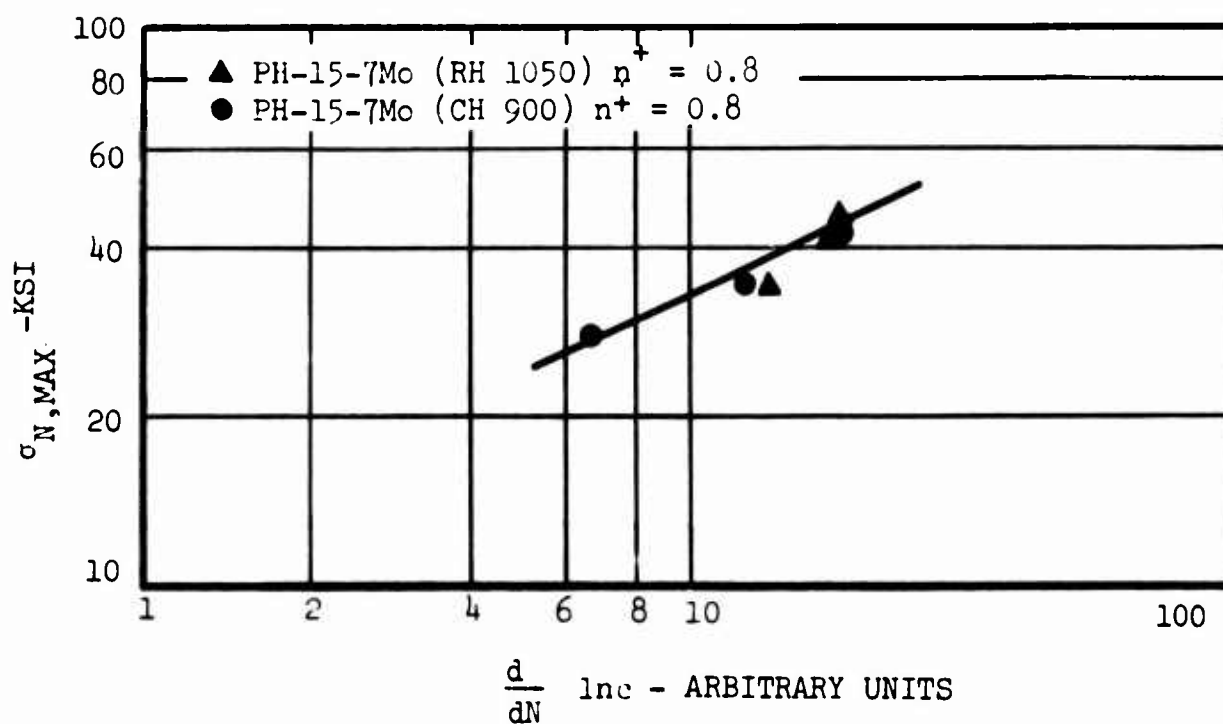
FOR D6AC AND HP9-4-25

FIG. 30 $\frac{d}{dN}$ Inc VS $\sigma_{N, MAX}$ CURVE FOR THE DETERMINATION OF n^+
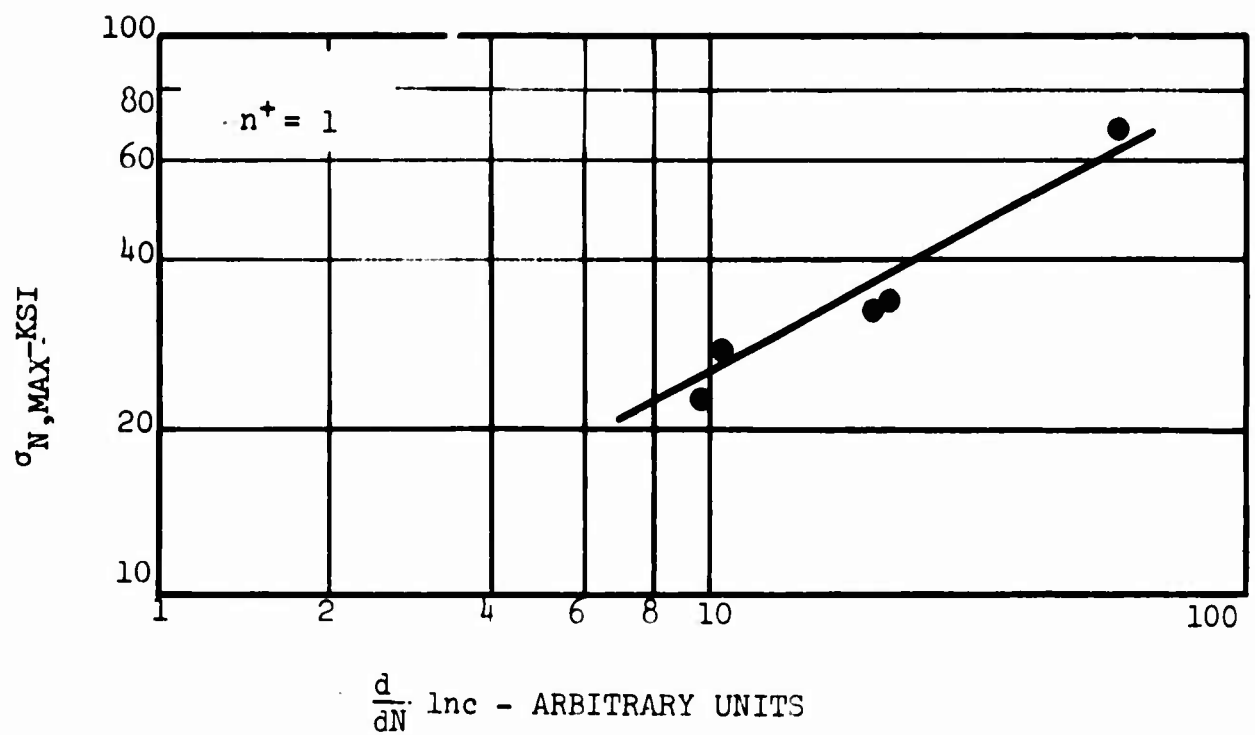
FOR PH-15-7Mo, CH 900 AND RH-1050 (SHARP NOTCH TESTS)

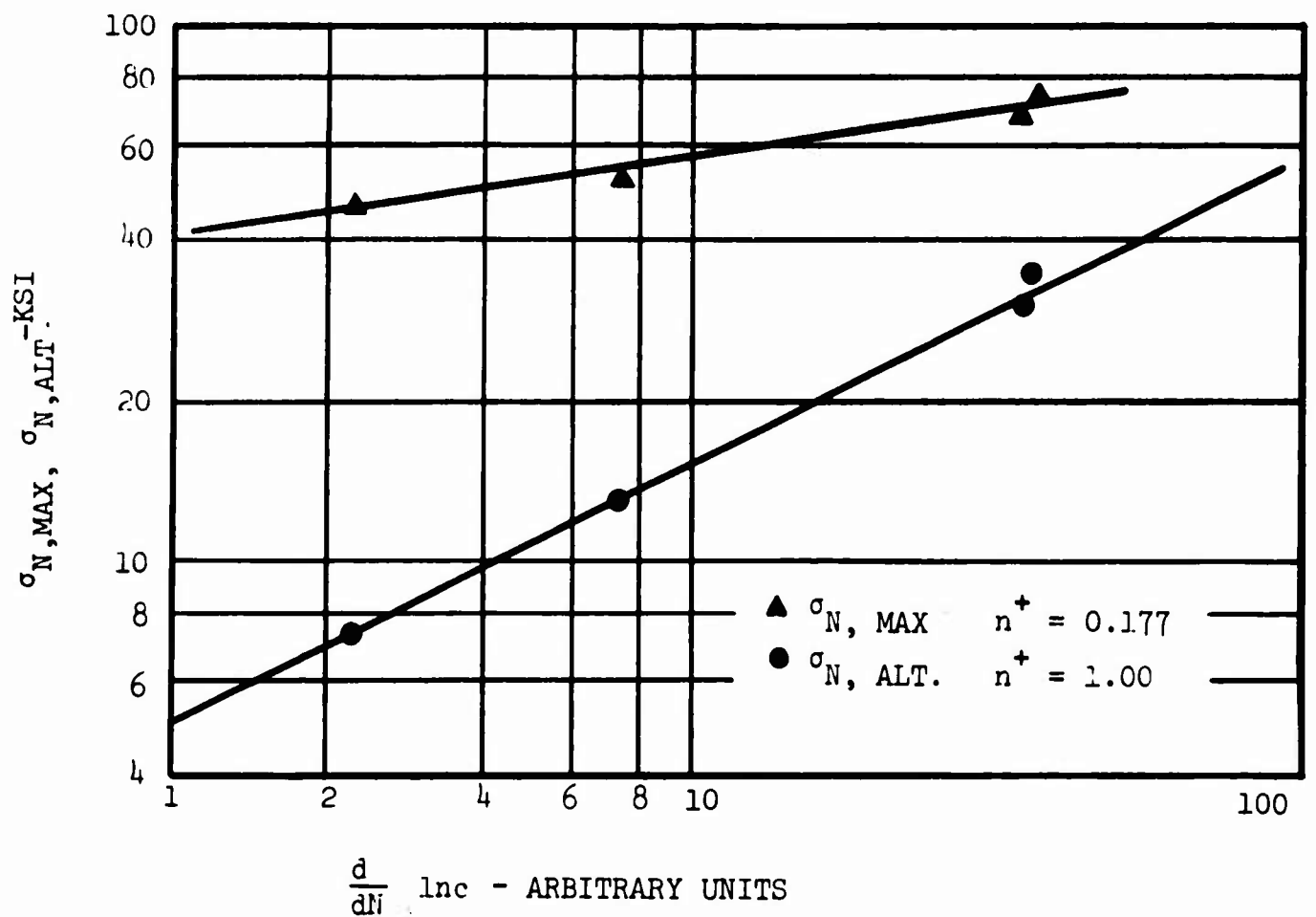FIG. 31 $\frac{d}{dN}$ lnc VS $\sigma_{N,\ MAX}$ CURVE FOR THE DETERMINATION OF n^+ FOR Ti-6Al-4V(SHARP NOTCH TESTS)

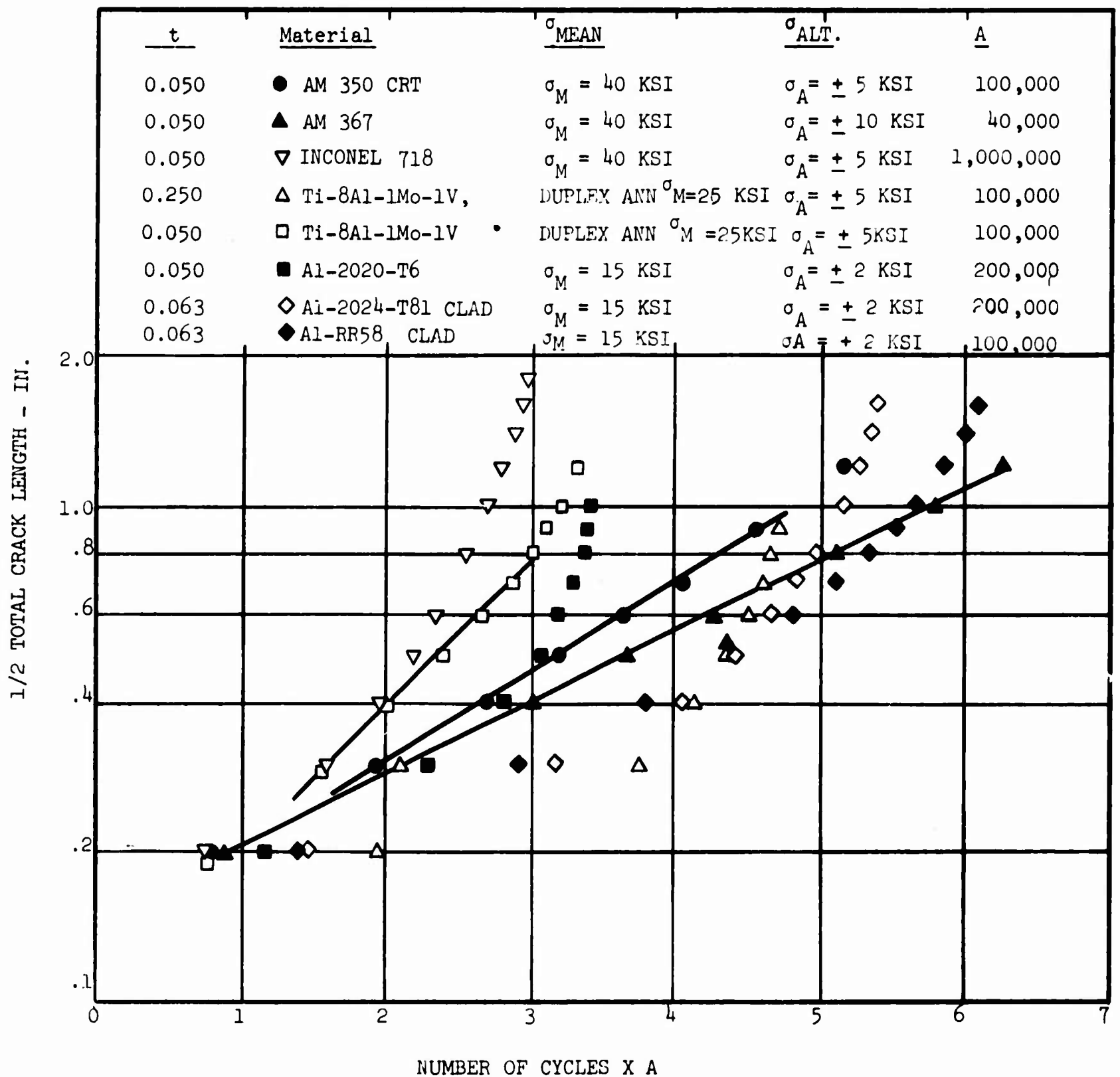FIG. 32 $\frac{d}{dN}$ lnc VS $\sigma_{N,\ MAX}$ AND $\sigma_{N,\ ALT.}$ FOR THE DETERMINATION OF n^+ FOR AISI 301

43

t	Material	σ_{MEAN}	$\sigma_{ALT.}$	A
0.050	● AM 350 CRT	σ_M = 40 KSI	σ_A = ± 5 KSI	100,000
0.050	▲ AM 367	σ_M = 40 KSI	σ_A = ± 10 KSI	40,000
0.050	▽ INCONEL 718	σ_M = 40 KSI	σ_A = ± 5 KSI	1,000,000
0.250	△ Ti-8Al-1Mo-1V,	DUPLEX ANN σ_M=25 KSI	σ_A = ± 5 KSI	100,000
0.050	□ Ti-8Al-1Mo-1V ·	DUPLEX ANN σ_M =25KSI	σ_A = ± 5KSI	100,000
0.050	■ Al-2020-T6	σ_M = 15 KSI	σ_A = ± 2 KSI	200,000
0.063	◇ Al-2024-T81 CLAD	σ_M = 15 KSI	σ_A = ± 2 KSI	200,000
0.063	◆ Al-RR58 CLAD	σ_M = 15 KSI	σ_A = ± 2 KSI	100,000

1/2 TOTAL CRACK LENGTH - IN.

NUMBER OF CYCLES X A

FIG. 33 CRACK LENGTH VS NUMBER OF CYCLES FOR MATERIALS TESTED AT NASA (25)

44
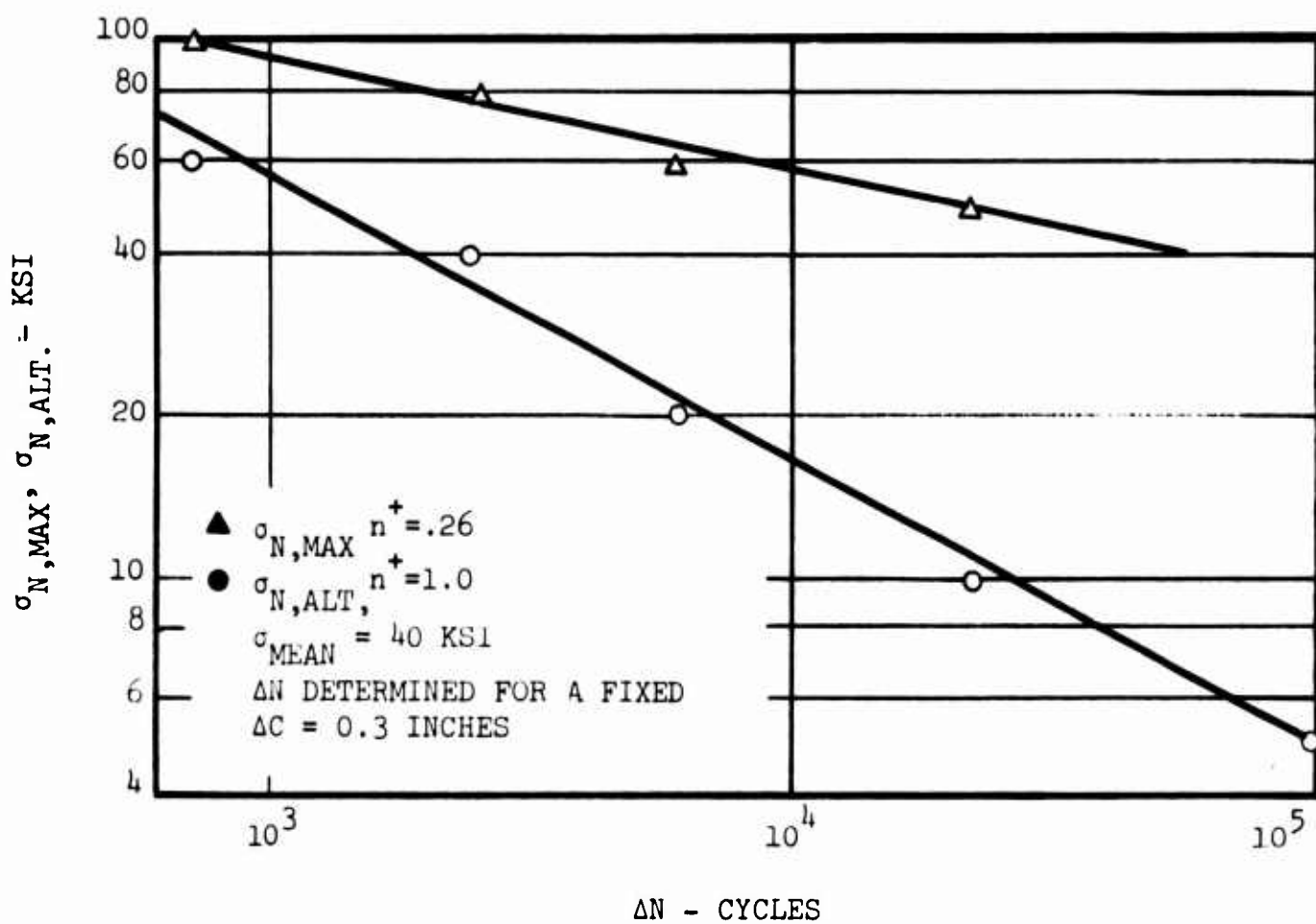
FIG. 34 σ_N VS ΔN CURVE FOR A FIXED ΔC FOR DETERMINATION OF n^+
VALUES FOR AM-350 (CRT). (NASA DATA)
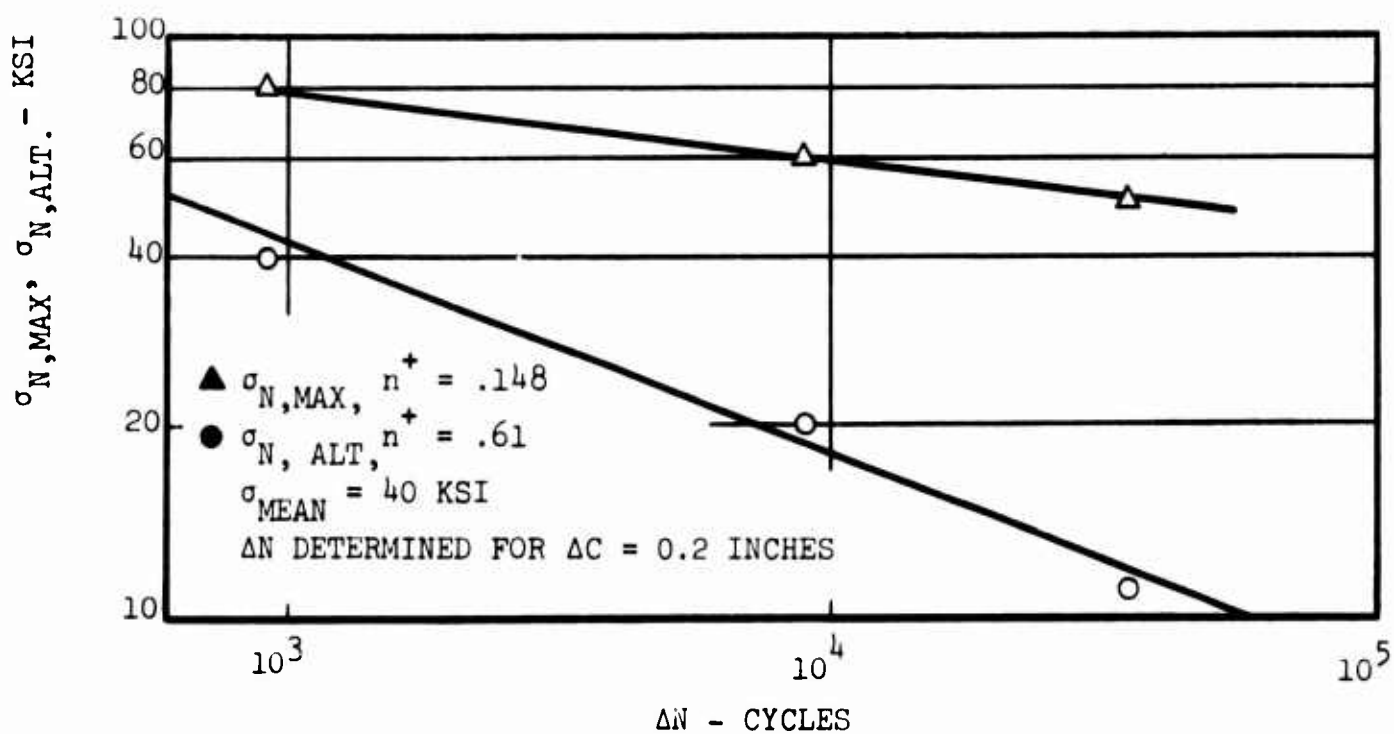
FIG. 35 σ_N VS ΔN CURVE FOR A FIXED ΔC FOR DETERMINATION OF n^+
VALUES FOR AM-367. (NASA DATA)
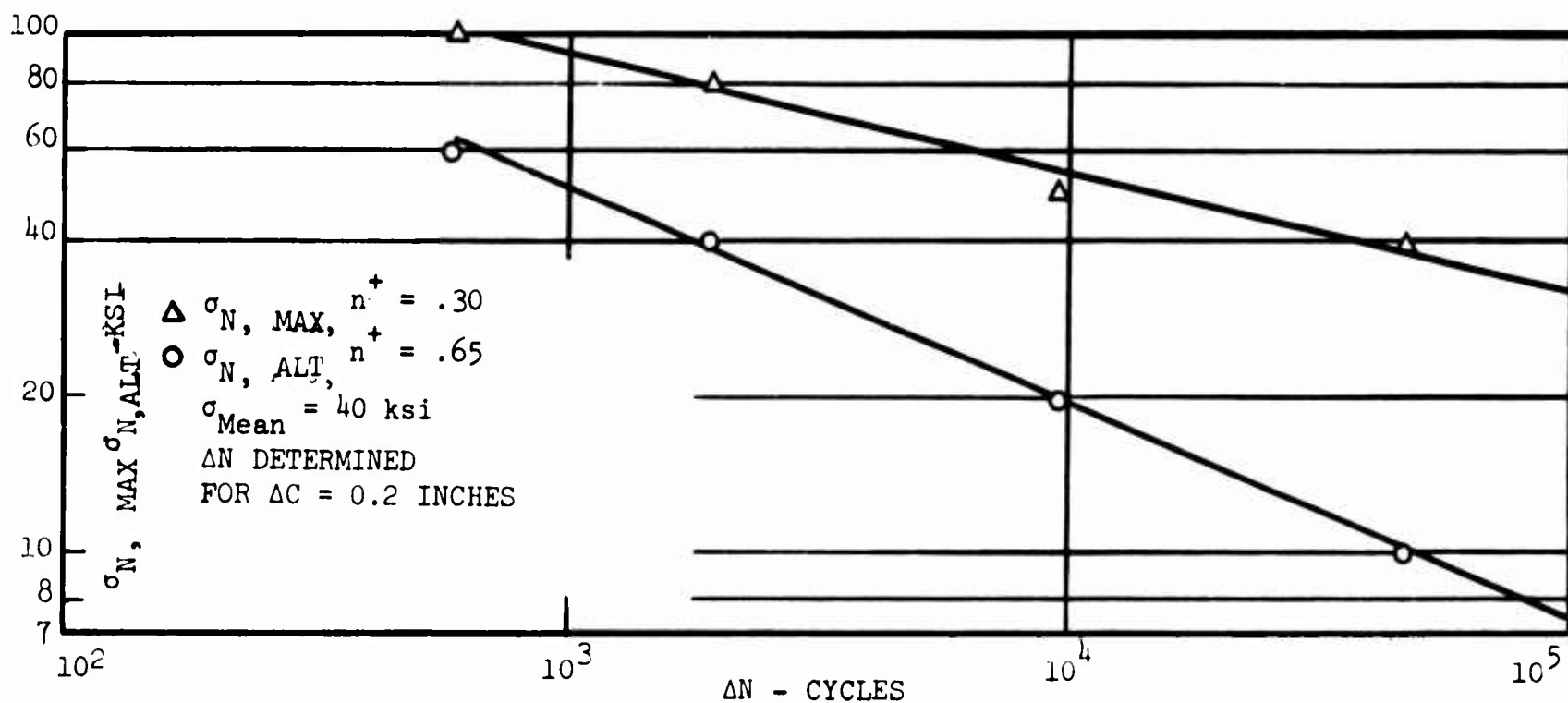
FIG. 36 σ_N VS ΔN CURVE FOR A FIXED ΔC FOR DETERMINATION OF n^+ VALUES FOR INCONEL 718

(NASA DATA)
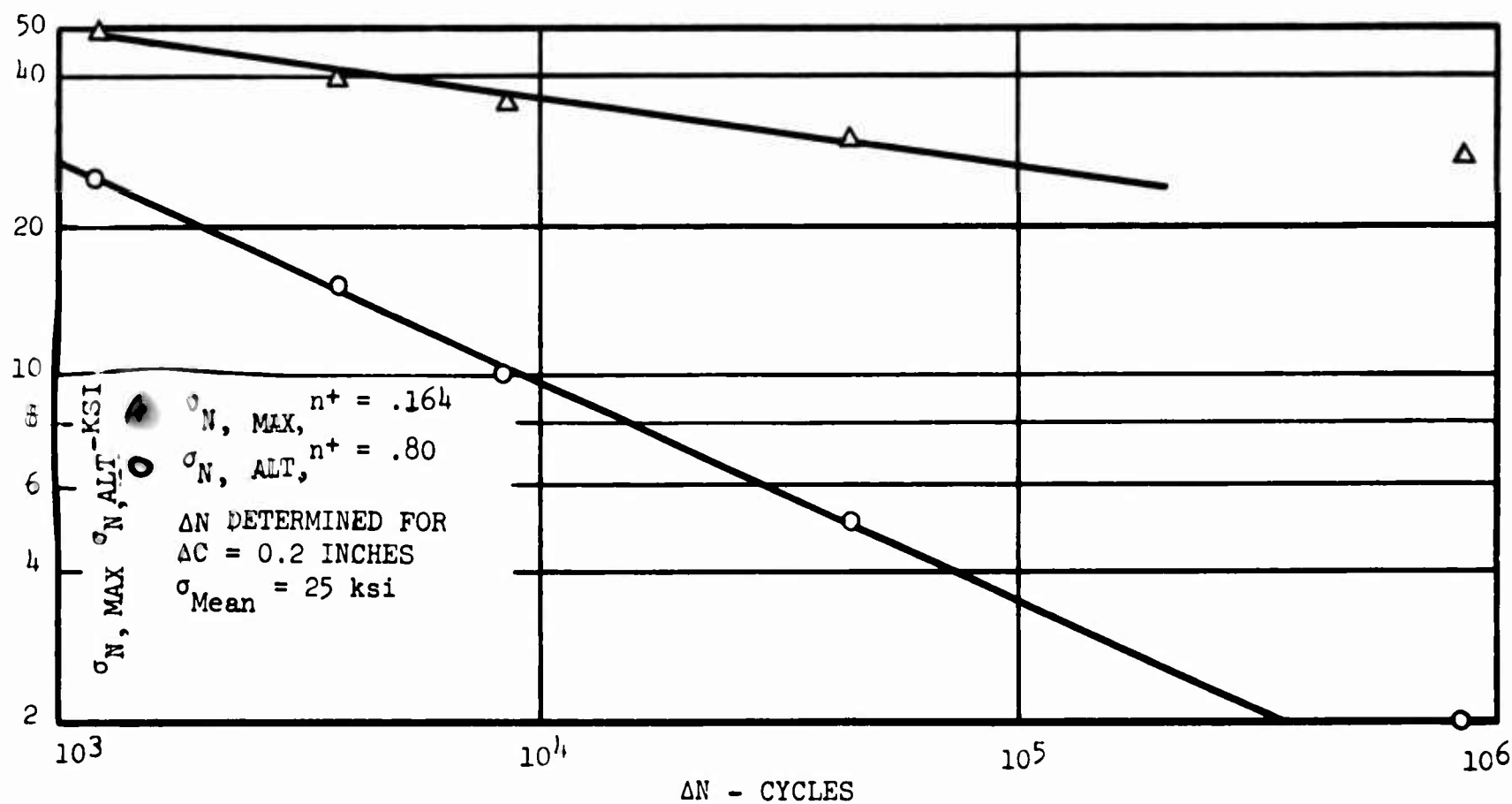
FIG. 37 σ_N VS ΔN CURVE FOR A FIXED ΔC FOR DETERMINATION OF n^+ VALUES FOR Ti-8A1-1Mo-1V

(0.050 IN THICK) (NASA DATA)

46
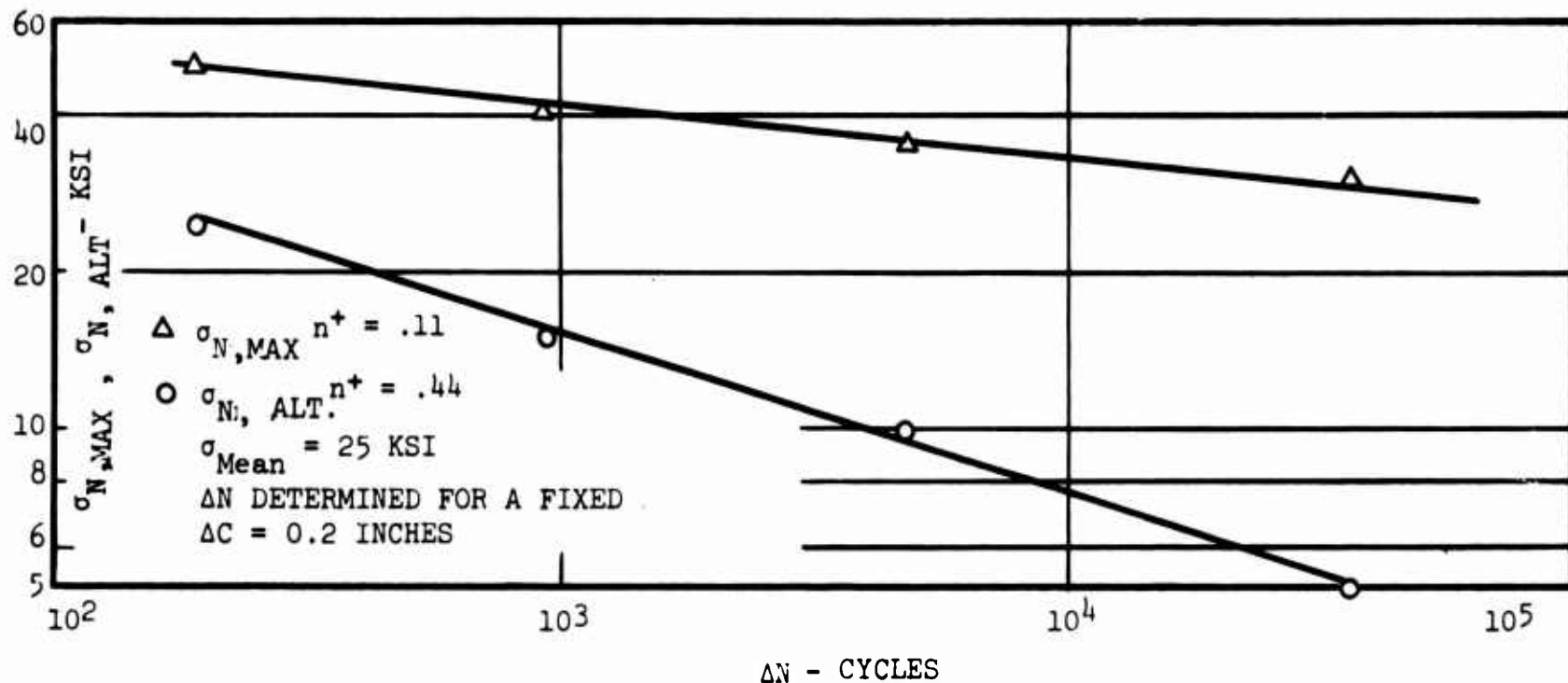
FIG. 38 σ_N VS ΔN CURVE FOR A FIXED ΔC FOR DETERMINATION OF n^+ VALUFS FOR Ti-8A1-1Mo-1V (0.250 IN. THICK) (NASA DATA)
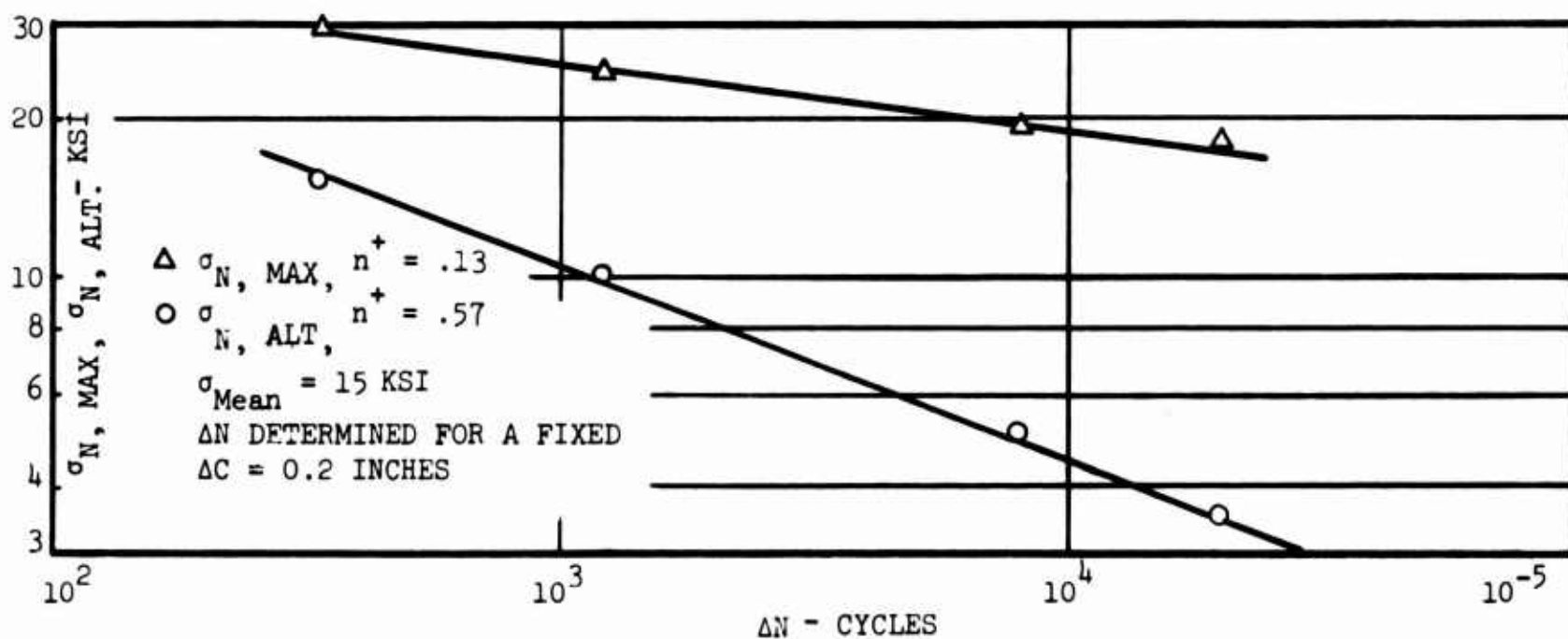
FIG. 39 σ_N VS ΔN CURVE FOR A FIXED ΔC FOR DETERMINATION OF n^+ VALUES FOR 2024-T81.

(CLAD) (NASA DATA)

47

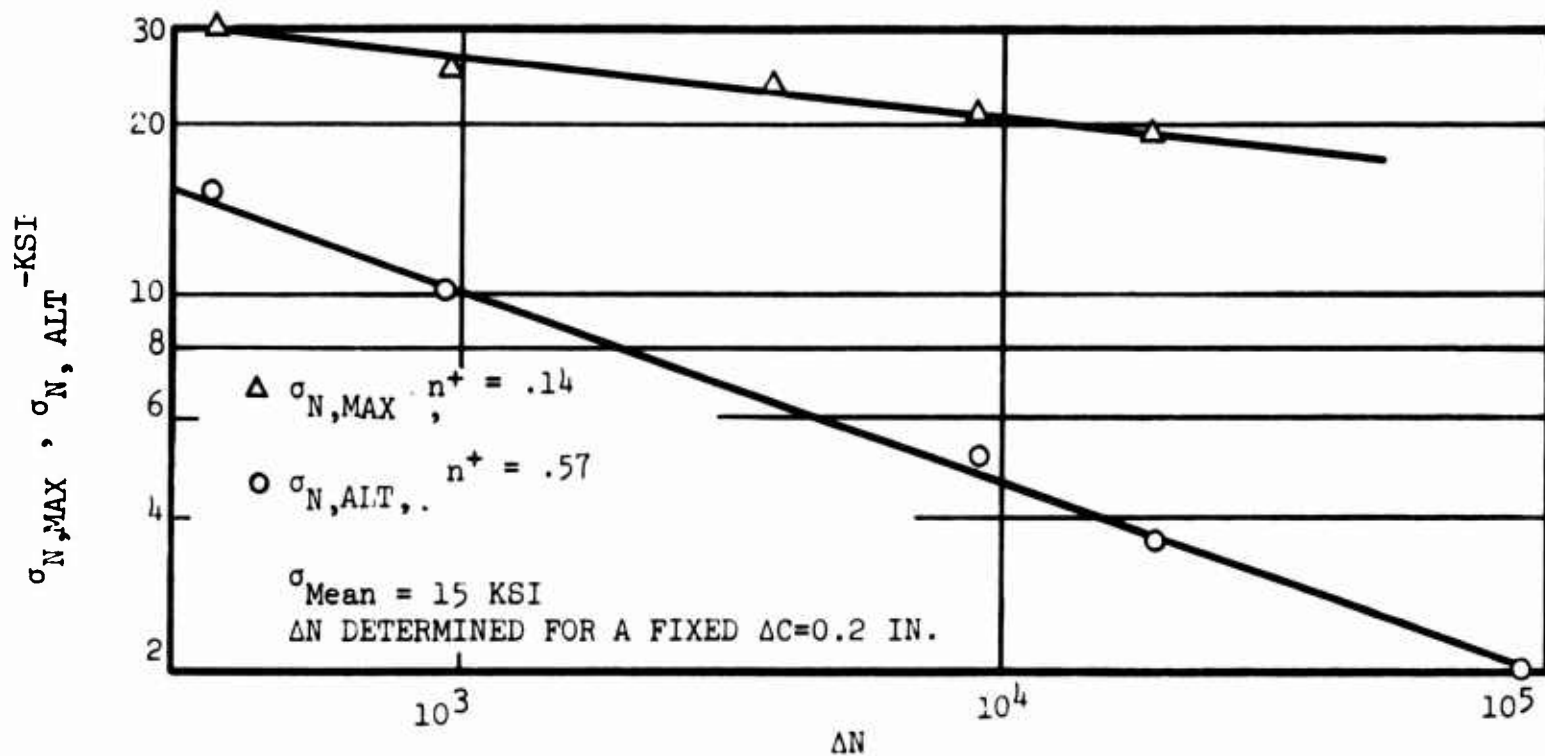FIG. 40 σ_N VS ΔN CURVE FOR A FIXED ΔC FOR DETERMINATION OF n^+ VALUES FOR

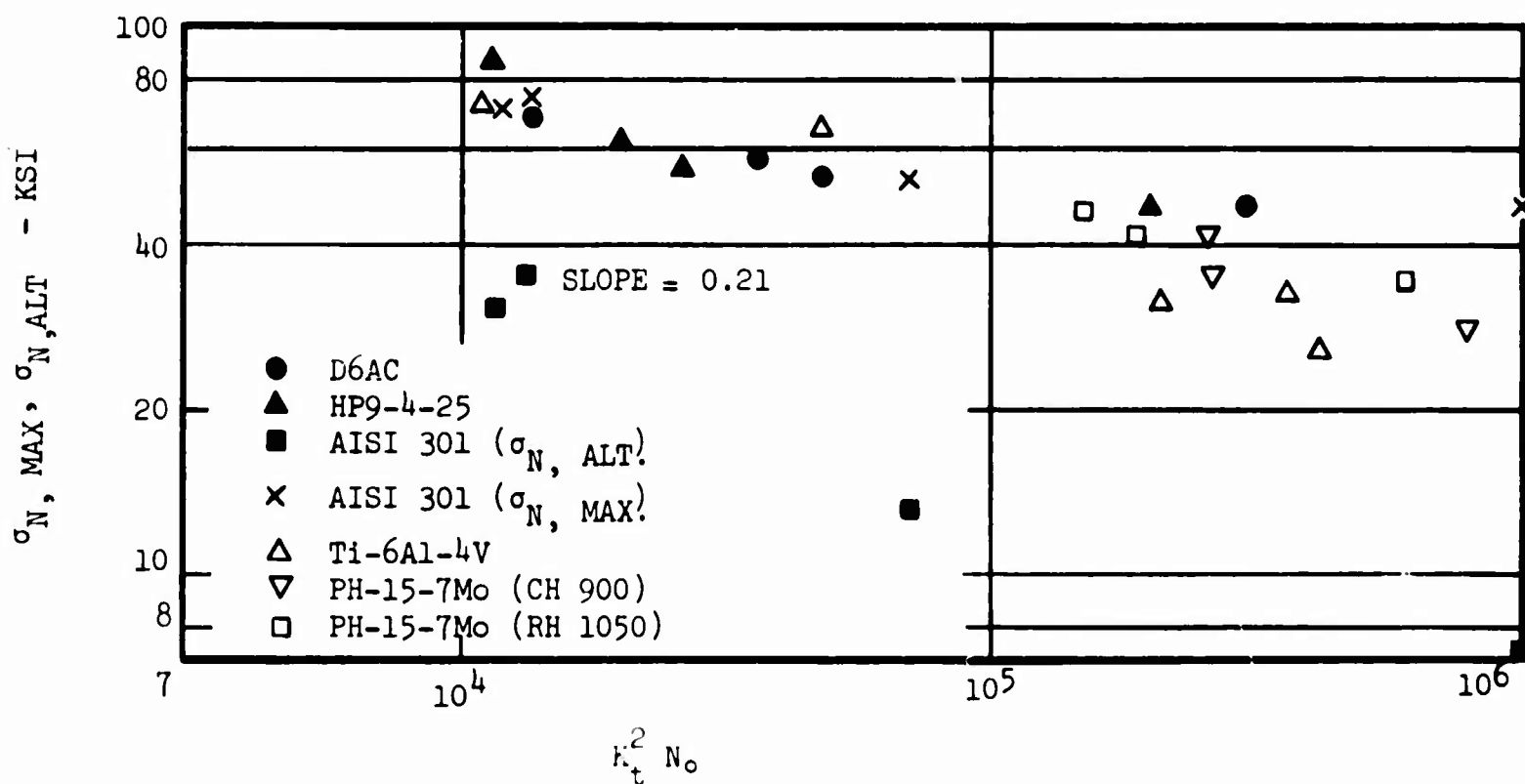RR-58 (CLAD)   (NASA DATA)

FIG. 41 σ_N VS ($K_t^2 N_o$) CURVE FOR ALL MATERIALS TESTED IN THE PRESENT

STUDY